



Geologic Map of the Providence Mountains in Parts of the Fountain Peak and Adjacent 7.5' Quadrangles, San Bernardino County, California

By Paul Stone, David M. Miller, Calvin H. Stevens, Jose Rosario, Jorge A. Vazquez, Elmira Wan, Susan S. Priest, and Zenon C. Valin

Pamphlet to accompany

Scientific Investigations Map 3376



2017

U.S. Department of the Interior
U.S. Geological Survey

U.S. Department of the Interior

RYAN K. ZINKE, Secretary

U.S. Geological Survey

William H. Werkheiser, Acting Director

U.S. Geological Survey, Reston, Virginia: 2017

For more information on the USGS—the Federal source for science about the Earth, its natural and living resources, natural hazards, and the environment—visit <http://www.usgs.gov> or call 1–888–ASK–USGS

For an overview of USGS information products, including maps, imagery, and publications, visit <http://store.usgs.gov>

To order this and other USGS information products, visit <http://store.usgs.gov>

Any use of trade, firm, or product names is for descriptive purposes only and does not imply endorsement by the U.S. Government.

Although this information product, for the most part, is in the public domain, it also may contain copyrighted materials as noted in the text. Permission to reproduce copyrighted items must be secured from the copyright owner.

Suggested citation:

Stone, Paul, Miller, D.M., Stevens, C.H., Rosario, Jose, Vazquez, J.A., Wan, Elmira, Priest, S.S., and Valin, Z.C., 2017, Geologic map of the Providence Mountains in parts of the Fountain Peak and adjacent 7.5' quadrangles, San Bernardino County, California: U.S. Geological Survey Scientific Investigations Map 3376, 52 p., <https://doi.org/10.3133/sim3376>.

ISSN 2329–132X (online)

Cover photograph:

View southeast to Providence Mountains, California, showing a thick sequence of Neoproterozoic to Paleozoic sedimentary rocks. Brown rocks at base of range are Neoproterozoic to Cambrian quartzite that overlies Paleoproterozoic metamorphic rocks; cliff-forming, light-colored rocks above are primarily Cambrian to Permian dolomite and limestone. Latest Pleistocene to Holocene alluvial deposits in foreground.

Contents

Introduction	1
Previous Studies	1
Methods of Study	4
Stratigraphy and Lithology.....	4
Paleoproterozoic Basement Rocks.....	4
Neoproterozoic to Triassic Sedimentary Rocks	4
Triassic or Jurassic Conglomerate	6
Jurassic Fountain Peak Rhyolite	6
Jurassic Plutonic Rocks.....	9
Jurassic Dikes	10
Age Relations of Jurassic Igneous Rocks	12
Miocene Volcanic Rocks	13
Pliocene(?) and Quaternary Surficial Deposits	14
Structure	15
Geologic History and Regional Relations.....	17
DESCRIPTION OF MAP UNITS	19
References Cited	34
Appendix 1—Sample Localities and Descriptions	38
Appendix 2—Fossil Identifications	39
Appendix 3—Geochemical Data	41
Appendix 4—Geochronologic Data	46
Appendix 5—Tephrochronologic Analysis.....	51
Introduction.....	51
Sample Descriptions.....	51
Analysis.....	52

Figures

Figure 1. Map showing location of geologic map area.....	2
Figure 2. Map showing selected geographic features in geologic map area.....	3
Figure 3. Chart comparing units recognized in this report with those of Hazzard (1954) and Palmer and Hazzard (1956).....	5
Figure 4. Reduced-scale geologic map of study area showing Jurassic rock units and major faults. Jurassic units are as follows: Jbw, monzogranite of Bonanza King Wash; Jt, monzogranite of Tough Nut Spring; Jg, Jgg, Jgs, Jgqm, Jgm, Jgmr, Jgr, subunits of quartz monzonite of Goldstone; Jfr, Jfs, subunits of Fountain Peak Rhyolite. See full-scale map and Description of Map Units for details.....	7
Figure 5. Total alkali-silica (TAS) plot showing geochemical composition of unit Jfr of Fountain Peak Rhyolite. Compositional fields from Best and Christiansen (2001) and LeMaitre and others (2002). Analytical data normalized to 100 percent (volatile-free). See appendix 3 for geochemical data.....	8
Figure 6. Total alkali-silica (TAS) plot showing geochemical compositions of plutonic rocks in map area. Compositional fields from Best and Christiansen (2001) and LeMaitre and others (2002). Analytical data normalized to 100 percent (volatile-free). See appendix 3 for geochemical data.....	10
Figure 7. Total alkali-silica (TAS) plot showing geochemical compositions of felsic to intermediate dikes (unit Jdf) in map area. Compositional fields from Best and Christiansen (2001) and LeMaitre and others (2002). Analytical data normalized to 100 percent (volatile-free). See appendix 3 for geochemical data.....	11

Figure 8.	Weighted mean $^{206}\text{Pb}^*/^{238}\text{U}$ ages of individual zircon grains from analyzed Jurassic igneous rocks. For this diagram, data from plutons, Fountain Peak Rhyolite, and felsic to intermediate dikes were statistically analyzed together using Isoplot (Ludwig, 2008). Diagram shows that samples of all three rock types are of very similar age, with a mean of about 163.5 Ma. Bars depict 2-sigma errors; boxes show weighted mean crystallization ages, mean square weighted deviation (MSWD), and probability of fit. See appendix 4 for weighted mean ages of individual samples.....	12
Figure 9.	Total alkali-silica (TAS) plot showing geochemical compositions of Miocene volcanic rocks (Peach Spring Tuff and Wild Horse Mesa Tuff) in and near map area. Compositional fields from Best and Christiansen (2001) and LeMaitre and others (2002). Analytical data normalized to 100 percent (volatile-free). See appendix 3 for geochemical data.....	13
Figure 10.	Harker diagram showing high titanium (TiO_2) vs. silica (SiO_2) content of Peach Spring Tuff (unit Tp) relative to that of most units of Wild Horse Mesa Tuff (units Tw1, Tw2u, Tw2w, Tw3). Titanium content of unit Tw4 is comparable to that of Peach Spring Tuff. Analytical data normalized to 100 percent (volatile-free). See appendix 3 for geochemical data.....	14
Figure 11.	Thin-section photographs of fusulinids from the Bird Spring Formation. All figures are axial sections. Specimens are housed in San Jose State University Museum of Paleontology, San Jose, California. A, <i>Leptotriticites</i> sp., sample S-2112. B, C, <i>Leptotriticites</i> cf. <i>L. californicus</i> , sample S-2112. D, <i>Leptotriticites</i> cf. <i>L. panamintensis</i> , sample S-2112. E, F, <i>Schwagerina providens</i> , sample S-2048. G, <i>Schwagerina aculeata</i> , sample S-2116. H, <i>Schwagerina aculeata?</i> , sample S-2115. I, <i>Schwagerina aculeata</i> , sample S-2110. J, <i>Schwagerina aculeata</i> , sample S-2036. K, <i>Schwagerina aculeata</i> , sample S-2110. L, <i>Schwagerina aculeata</i> , sample S-2116. M, <i>Schwagerina</i> sp. 4 of Stevens and Stone (2007), sample S-2114. N, <i>Schwagerina wellsensis</i> , sample S-2091. O, <i>Stewartina</i> sp., sample S-2113. P, <i>Pseudoschwagerina roeseleri</i> , sample S-2110. Q, <i>Pseudoschwagerina roeseleri</i> , sample S-2091.	40
Figure 12.	Harker diagrams showing variations in the abundances of selected oxides with respect to silica (SiO_2) in samples from Jurassic map unit Jfr (Fountain Peak Rhyolite). Oxides are titanium (TiO_2), aluminum (Al_2O_3), iron (Fe_2O_3), magnesium (MgO), calcium (CaO), potassium (K_2O), sodium (Na_2O), and potassium + sodium ($\text{K}_2\text{O}+\text{Na}_2\text{O}$). Values are in normalized weight percent.....	42
Figure 13.	Harker diagrams showing variations in the abundances of selected oxides with respect to silica (SiO_2) in samples from Jurassic plutonic map units Jg, Jgg, Jgm, Jgmr, Jgqm, Jgr, Jgs, Jt, and Jbw (see Description of Map Units for unit names). Oxides are titanium (TiO_2), aluminum (Al_2O_3), iron (Fe_2O_3), magnesium (MgO), calcium (CaO), potassium (K_2O), sodium (Na_2O), and potassium + sodium ($\text{K}_2\text{O}+\text{Na}_2\text{O}$). Values are in normalized weight percent.	43
Figure 14.	Harker diagrams showing variations in the abundances of selected oxides with respect to silica (SiO_2) in samples from Jurassic map unit Jdf (felsic to intermediate dikes). Oxides are titanium (TiO_2), aluminum (Al_2O_3), iron (Fe_2O_3), magnesium (MgO), calcium (CaO), potassium (K_2O), sodium (Na_2O), and potassium + sodium ($\text{K}_2\text{O}+\text{Na}_2\text{O}$). Values are in normalized weight percent.....	44
Figure 15.	Harker diagrams showing variations in the abundances of selected oxides with respect to silica (SiO_2) in samples from Miocene volcanic map units Tp (Peach Spring Tuff) and Tw1, Tw2u, Tw2w, Tw3, and Tw4 (subunits of Wild Horse Mesa Tuff). Oxides are titanium (TiO_2), aluminum (Al_2O_3), iron (Fe_2O_3), magnesium (MgO), calcium (CaO), potassium (K_2O), sodium (Na_2O), and potassium + sodium ($\text{K}_2\text{O}+\text{Na}_2\text{O}$). Values are in normalized weight percent.	45
Figure 16.	Reduced-scale geologic map showing locations of analyzed geochronologic samples (circles) and tephrochronologic samples (triangles). Note locations of geochronologic samples 14-PR-5021 (unit Jt) and 14-PR-5023 (unit Jdf) north of the geologic map area.....	47
Figure 17.	Weighted mean $^{206}\text{Pb}^*/^{238}\text{U}$ ages for samples 12-PR-3701 (unit Jgqm), 12-PR-3706 (unit Jgm), and 12-PR-3713 (unit Jfr). Bars depict 2-sigma errors; boxes show weighted mean crystallization ages, mean square weighted deviation (MSWD), and probability of fit. See table 6 for data.	48

Figure 18. Weighted mean $^{206}\text{Pb}^*/^{238}\text{U}$ ages for samples 12-PR-3888 (unit Jdf), 12-PR-3889 (unit Jfr), and 13-PR-4854 (unit Jbw). Bars depict 2-sigma errors; boxes show weighted mean crystallization ages, mean square weighted deviation (MSWD), and probability of fit. See table 6 for data. 49

Figure 19. Weighted mean $^{206}\text{Pb}^*/^{238}\text{U}$ ages for samples 14-PR-5021 (unit Jt), 14-PR-5023 (unit Jdf), and 14-PR-5248 (unit Jg). Bars depict 2-sigma errors; boxes show weighted mean crystallization ages, mean square weighted deviation (MSWD), and probability of fit. See table 6 for data. 50

Tables

Table 1. Summary of U-Pb zircon ages of selected Jurassic igneous rocks from the Providence Mountains in and near the Fountain Peak and adjacent 7.5' quadrangles, San Bernardino County, California..... 8

Table 2. Localities and descriptions of samples from the Providence Mountains in parts of the Fountain Peak and adjacent 7.5' quadrangles, San Bernardino County, California. [Title of table is included here for continuity; complete table is available at <https://doi.org/10.3133/sim3376>.]..... 38

Table 3. Fusulinids from the Bird Spring Formation in the Providence Mountains in parts of the Fountain Peak and adjacent 7.5' quadrangles, San Bernardino County, California..... 39

Table 4. X-ray fluorescence geochemical analyses of selected Jurassic and Miocene igneous rock samples from the Providence Mountains in parts of the Fountain Peak and adjacent 7.5' quadrangles, San Bernardino County, California. [Title of table is included here for continuity; complete table is available at <https://doi.org/10.3133/sim3376>.] 41

Table 5. ICP-AES (inductively coupled plasma atomic emission spectrometry) geochemical analyses of selected Jurassic and Miocene igneous rock samples from the Providence Mountains in parts of the Fountain Peak and adjacent 7.5' quadrangles, San Bernardino County, California. [Title of table is included here for continuity; complete table is available at <https://doi.org/10.3133/sim3376>.] 41

Table 6. SHRIMP-RG U-PB zircon data for selected Jurassic igneous rock samples from the Providence Mountains in parts of the Fountain Peak and adjacent 7.5' quadrangles, San Bernardino County, California. [Title of table is included here for continuity; complete table is available at <https://doi.org/10.3133/sim3376>.] 46

Table 7. Summary of chemical compositions of glass from tuff samples, Providence Mountains in parts of the Fountain Peak and adjacent 7.5' quadrangles, San Bernardino County, California, determined by microprobe analysis..... 51

Table 8. Chemical compositions of individual glass shards from tuff samples, Providence Mountains in parts of the Fountain Peak and adjacent 7.5' quadrangles, San Bernardino County, California, determined by microprobe analysis. [Title of table is included here for continuity; complete table is available at <https://doi.org/10.3133/sim3376>.] 51

Geologic Map of the Providence Mountains in Parts of the Fountain Peak and Adjacent 7.5' Quadrangles, San Bernardino County, California

By Paul Stone,¹ David M. Miller,¹ Calvin H. Stevens,² Jose Rosario,¹ Jorge A. Vazquez,¹ Elmira Wan,¹ Susan S. Priest,¹ and Zenon C. Valin¹

Introduction

The Providence Mountains are in the eastern Mojave Desert about 60 km southeast of Baker, San Bernardino County, California (fig. 1). This range, which is noted for its prominent cliffs of Paleozoic limestone, is part of a northeast-trending belt of mountainous terrain more than 100 km long that also includes the Granite Mountains, Mid Hills, and New York Mountains. Providence Mountains State Recreation Area encompasses part of the range, the remainder of which is within Mojave National Preserve, a large parcel of land administered by the National Park Service (fig. 1). Access to the Providence Mountains is by secondary roads leading south and north from Interstate Highways 15 and 40, respectively, which bound the main part of Mojave National Preserve.

The geologic map presented here includes most of Providence Mountains State Recreation Area and land that surrounds it on the north, west, and south (fig. 2). This area covers most of the Fountain Peak 7.5' quadrangle and small adjacent parts of the Hayden quadrangle to the north, the Columbia Mountain quadrangle to the northeast, and the Colton Well quadrangle to the east. The map area includes representative outcrops of most of the major geologic elements of the Providence Mountains, including gneissic Paleoproterozoic basement rocks, a thick overlying sequence of Neoproterozoic to Triassic sedimentary rocks, Jurassic rhyolite that intrudes and overlies the sedimentary rocks, Jurassic plutons and associated dikes, Miocene volcanic rocks, and a variety of Quaternary surficial deposits derived from local bedrock units. The purpose of the project was to map the area in detail, with primary emphasis on the pre-Quaternary units, to provide an improved stratigraphic, structural, and geochronologic framework for use in land management applications and scientific research.

This project was funded by the National Cooperative Geologic Mapping Program of the U.S. Geological Survey and was coordinated with Mojave National Preserve and Providence Mountains State Recreation Area. Debra Hughson (Mojave National Preserve) and Darrell Bennett and Andrew Fitzpatrick (Providence Mountains State Recreation Area) coordinated the field work on behalf of their respective agencies, and Ted Weasma (Mojave National Preserve) spent several days in the field with the senior author of this report.

Previous Studies

The earliest significant geologic investigations of the Providence Mountains were by J.C. Hazzard and colleagues. This work began with stratigraphic and paleontological studies of selected

¹ U.S. Geological Survey

² San Jose State University

Paleozoic units (Hazzard and Crickmay, 1933; Hazzard and Mason, 1936; Thompson and Hazzard, 1946) and culminated with a detailed geologic map and summary report (Hazzard, 1954) followed by final stratigraphic revisions (Palmer and Hazzard, 1956). Hewett (1956) mapped and synthesized the stratigraphy, structure, and mineral deposits of the Ivanpah 1° x 1° quadrangle, which includes the northern part of the Providence Mountains. Additional information on the Paleozoic stratigraphy of the Providence Mountains was later presented by Law (1969) and Stewart (1970).

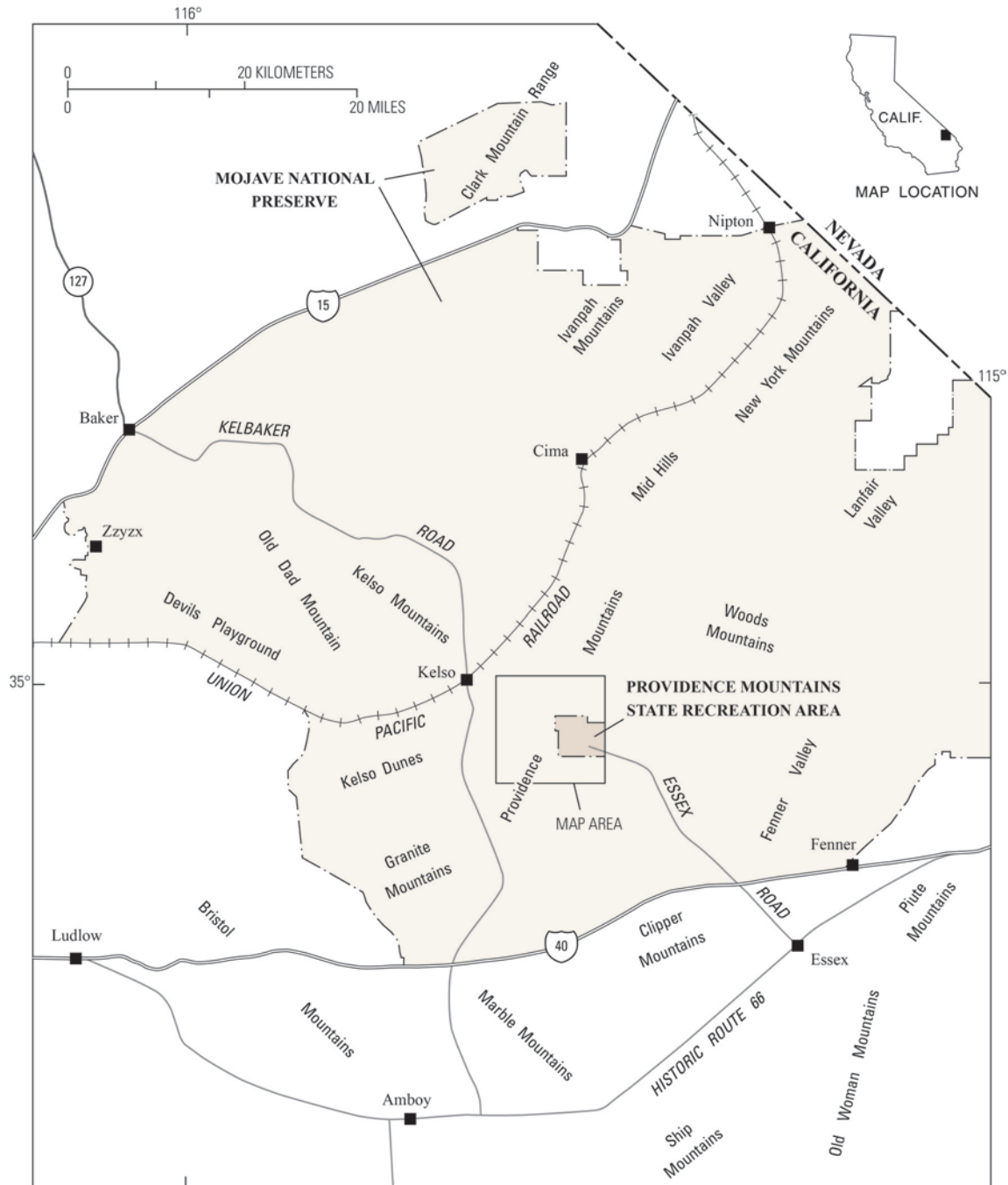


Figure 1. Map showing location of geologic map area.



Figure 2. Map showing selected geographic features in geologic map area.

In the 1980s, the Providence Mountains were included in a joint program of the U.S. Geological Survey and U.S. Bureau of Mines to investigate the geology and mineral-resource potential of lands then administered by the U.S. Bureau of Land Management. This work resulted in two comprehensive reports that included geologic maps (Miller and others, 1985; Goldfarb and others, 1988). Later, Miller and others (1991) compiled a preliminary geologic map of East Mojave National Scenic Area, which subsequently became Mojave National Preserve. A separate report on mineral resources of the area was published by the California Division of Mines and Geology (Lloyd, 1993), with references to numerous earlier reports on mineral resources and mining. The geology and mineral resources of the region were again reported by Theodore (2007); that study included an updated geologic map by Miller and others (2007).

Topical studies of Providence Mountains geology since 1980 include those of Miller (1983), McCurry (1985, 1988), Fox and Miller (1990), Wooden and Miller (1990), Buesch (1991, 1993), Wilson

(1994), McDonald and McFadden (1994), McDonald and others (1995), McCurry and others (1995), Miller and others (1996), and Stevens and Stone (2007). A geophysical investigation of Mojave National Preserve and adjacent areas was reported by Langenheim and others (2009). The surficial (Quaternary) geology of the Providence Mountains and the surrounding region was mapped at a scale of 1:100,000 by Bedford and others (2010) and Miller (2012).

Methods of Study

Geologic features were mapped on color aerial photographs (stereoscopic photo pairs) at scales of 1:20,000 and 1:24,000. All map data are original to this study, although previous maps and reports were consulted frequently during the course of field work. Mapping was manually compiled on a printed topographic base map at a scale of 1:24,000 using a Kern PG-2 plotter, then scanned and digitized. More than 5,200 GPS waypoints were recorded during the course of field mapping to ensure locational accuracy of geologic features and samples. Most Quaternary features and inaccessible bedrock features were mapped entirely by interpretation of aerial photographs. Rock samples (appendix 1) were collected at 466 localities for the purposes of lithologic characterization (see Description of Map Units), fossil identification (appendix 2), geochemical analysis (appendix 3), geochronologic analysis (appendix 4), and tephrochronologic analysis (appendix 5).

Stratigraphy and Lithology

Paleoproterozoic Basement Rocks

The oldest rocks exposed in the study area are Paleoproterozoic metamorphic rocks (unit Xm). These rocks, which are most continuously exposed near the north margin of the area, are composed mainly of strongly foliated, quartzofeldspathic gneiss of probable granitic origin but also include fine-grained, quartz-rich rocks of possible sedimentary or volcanic origin. Wooden and Miller (1990) dated granitic gneiss a short distance to the north as $1,710 \pm 10$ Ma. Gneiss in the study area is cut by a few prominent quartz-rich veins or dikes (unit Xq) of unknown but presumed Paleoproterozoic age.

Neoproterozoic to Triassic Sedimentary Rocks

The metamorphic basement is nonconformably overlain by a thick sequence of sedimentary rocks that range from Neoproterozoic to Triassic. These rocks, which have a combined stratigraphic thickness of about 3.4 km, are herein divided into 13 first-order units. Many of these are the same as formations mapped by Hazzard (1954) and modified by Palmer and Hazzard (1956), but some differ as discussed below and shown in figure 3.

The lower, quartzitic part of the sequence is Neoproterozoic to Early Cambrian and was mapped as a single formation (Prospect Mountain Quartzite) by Hazzard (1954). These rocks are herein divided into three first-order units based on the detailed stratigraphic study of Stewart (1970): a lower unit assigned to the Johnnie Formation (unit Zj), a middle unit considered equivalent to the Stirling Quartzite and Wood Canyon Formation (unit Zu), and an upper unit assigned to the Zabriskie Quartzite (unit Z). The overlying, Early to Middle Cambrian formations—Latham Shale (unit Cl), Chambless Limestone (unit Ch), and Cadiz Formation (unit C)—are identical to those of Hazzard (1954), although a distinctive siltstone subunit (Cs) is recognized locally in the Cadiz Formation. The overlying Bonanza King Formation of Middle to Late Cambrian age also is identical to that of Hazzard (1954), although Hazzard's lower member is herein divided into the lower Papoose Lake Member (unit CbP) and upper Banded Mountain Member (unit CbB) of Barnes and others (1962). The overlying Silver King Dolomite Member (unit Cbs) and upper member (unit Cbu) of the Bonanza King Formation are identical to those of Hazzard (1954).

System	This report (showing thickness)		Hazzard (1954); Palmer and Hazzard (1956)	
Triassic	Moenkopi Formation (260 m)	limestone member (150 m)	Moenkopi Formation	
		sandstone member (110 m)		
Permian	Bird Spring Formation (975 m)		Bird Spring Formation	
Pennsylvanian				
Mississippian	Monte Cristo Limestone (250 m)		Monte Cristo Limestone	
Devonian	Limestone, dolomite, and quartzite (230 m)		Sultan Limestone	
Silurian(?)	Dolomite, sandy dolomite, and quartzite (390 m)			
Ordovician(?)			Dunderberg Shale (30 m)	
Cambrian	Bonanza King Formation (700 m)	upper member (80 m)		
		Silver King Member (100 m)	Silver King Member	
		Banded Mountain Member (300 m)	lower member	
		Papoose Lake Member (220 m)		
	Cadiz Formation (145 m)	Cadiz Formation		
	Chambless Limestone (65 m)	Chambless Limestone		
	Latham Shale (20 m)	Latham Shale		
	Zabriskie Quartzite (35 m)	Prospect Mountain Quartzite		
	Wood Canyon Formation and Stirling Quartzite, undivided (300 m)			
	Johnnie Formation (30 m)			
Neoproterozoic				

Figure 3. Chart comparing units recognized in this report with those of Hazzard (1954) and Palmer and Hazzard (1956).

Stratigraphically above the Bonanza King Formation are Late Cambrian to Devonian rocks assigned to the Cornfield Springs Formation and Sultan Limestone by Hazzard (1954) and Palmer and Hazzard (1956). These rocks are divided differently in this report. First, the lower, shale-rich part of the Cornfield Springs Formation is mapped separately as the regionally extensive Late Cambrian Dunderberg Shale (unit Cd). Second, we found during this study that the contact mapped by Hazzard (1954) between the Cornfield Springs Formation and the overlying Sultan Limestone is poorly defined

and inconsistent, leading to the conclusion that neither of these formation names can be definitively applied in the Providence Mountains. A prominent, stratigraphically higher contact does exist throughout the area, however, at the base of a cliff-forming limestone and dolomite sequence equivalent to the upper part of the Sultan Limestone. Therefore, in this report, the Late Cambrian to Devonian rocks that overlie the Dunderberg Shale are divided into two informal units: a lower unit (**DCd**) of Late Cambrian to Devonian dolomite, sandy dolomite, and quartzite, and an upper unit (**DI**) of Devonian limestone, dolomite, and quartzite. The lower unit may include Ordovician and Silurian rocks equivalent to those recognized in southern Nevada (Gans, 1974; Miller and Zilinsky, 1981). No sharp contact representing a regional Cambrian–Devonian unconformity such as that noted by Burchfiel and Davis (1981) is recognized in the study area.

Rocks above unit **DI** are here assigned to the Mississippian Monte Cristo Limestone (unit **Mm**), the Pennsylvanian and early Permian Bird Spring Formation (unit **PIPb**), and the Early Triassic Moenkopi Formation following the original usage of Hazzard (1954). The members of the Monte Cristo Limestone mapped by Hazzard (1954), however, were found to be inconsistently developed and are not mapped separately in this report. In addition, the Moenkopi Formation is divided into a lower sandstone member (unit **Tms**) and an upper limestone member (unit **Tml**) that were recognized but not mapped separately by Hazzard (1954).

Triassic or Jurassic Conglomerate

A thin layer of conglomerate containing abundant limestone clasts and subordinate sandstone clasts (unit **JRC**) overlies the Moenkopi Formation on the northwest flank of Edgar Peak (fig. 2). The stratigraphic position of this conglomerate beneath the Fountain Peak Rhyolite (see next section) restricts the age to Triassic or Jurassic. The clasts likely were derived by erosion of the Bird Spring and Moenkopi Formations, suggesting that the lower contact of the conglomerate is disconformable.

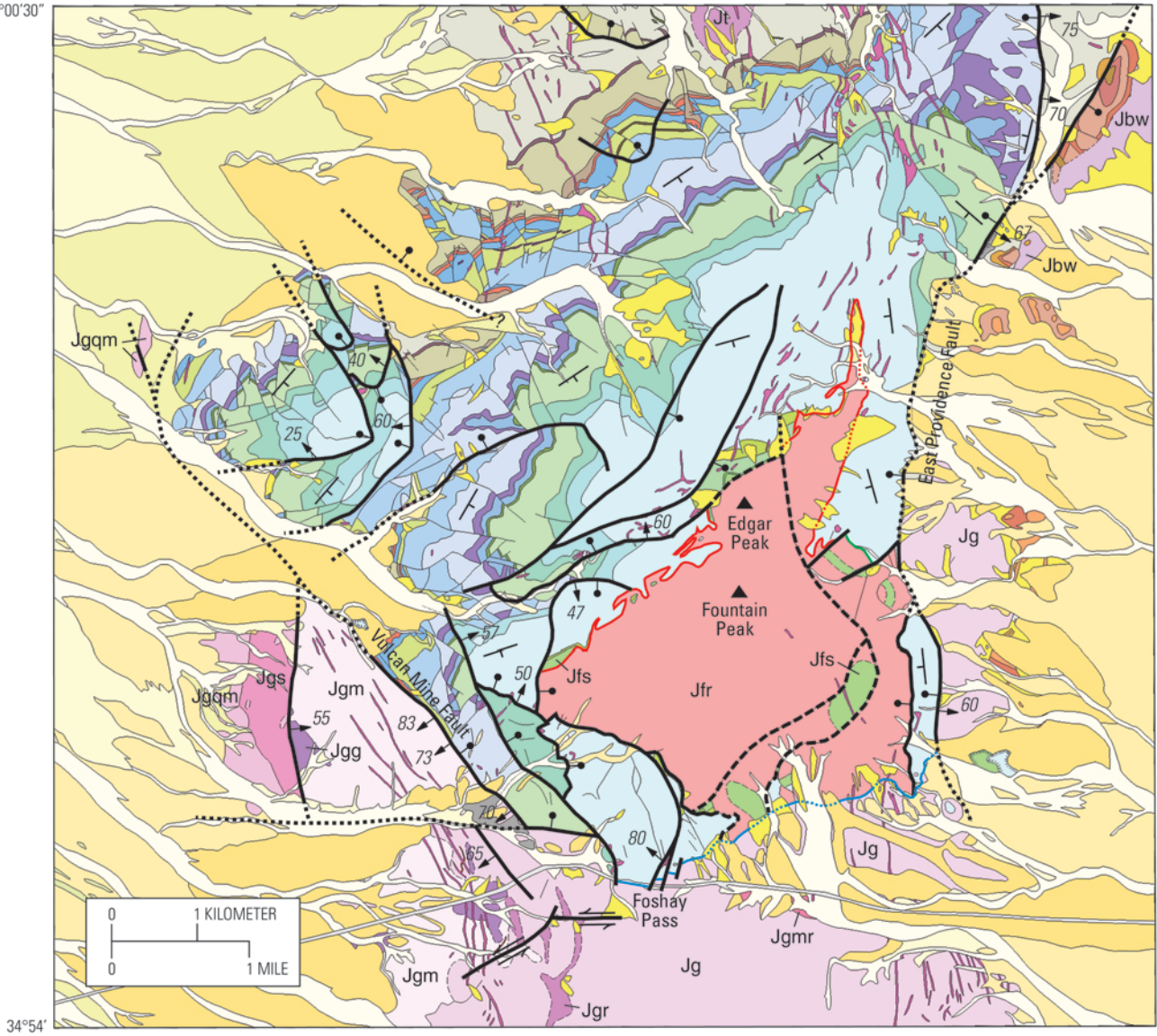
Jurassic Fountain Peak Rhyolite

A massive body of intrusive to extrusive rhyolite named the Fountain Peak Rhyolite by Hazzard (1954) crops out over a large part of the study area (fig. 4). This resistant rhyolite forms towering, reddish-brown crags that define the range crest in the vicinity of Fountain and Edgar Peaks. Sandstone, conglomerate, and tuff are locally exposed along contacts of the rhyolite with older rocks and within the rhyolite unit itself. Hazzard (1954) assigned both the rhyolite and the associated clastic rocks a Tertiary (Miocene?) age based on a tentative correlation with Miocene volcanic rocks exposed east of the Providence Mountains. Goldfarb and others (1988) alternatively suggested a Jurassic age for the rhyolite, although definitive evidence for this interpretation was lacking. Geochronologic analysis during the present study (appendix 4) confirms a late Middle to early Late Jurassic age for the rhyolite and, by inference, for the associated clastic rocks as well.

Hazzard (1954) mapped the Fountain Peak Rhyolite and the associated clastic rocks as separate units. Here, the Fountain Peak Rhyolite is considered to include both the rhyolite (unit **Jfr**) and the associated sandstone, conglomerate, and tuff (unit **Jfs**). An enigmatic limestone unit (**Jfl**) that forms a small outcrop about 1 km northwest of Blind Spring is also regarded as a subunit of the Fountain Peak Rhyolite because of its close spatial association with rocks of units **Jfr** and **Jfs**. Geochemical analysis confirms the rhyolitic composition of unit **Jfr** (fig. 5), and two samples from unit **Jfr** yield uranium-lead (U-Pb) zircon ages of about 164 Ma (table 1).

115°37'30"
35°00'30"

115°29'



34°54'

EXPLANATION

-  **Fault**—Dashed where inferred, dotted where concealed. Showing dip where known. Bar and ball on downthrown side. Arrows indicate lateral offset
-  **Depositional(?) contact of unit Jfr**
-  **Intrusive contact of unit Jfr**—Dotted where concealed
-  **Intrusive contact of unit Jg**—Dotted where concealed
-  **General direction of strike and dip of bedding**

Figure 4. Reduced-scale geologic map of study area showing Jurassic rock units and major faults. Jurassic units are as follows: Jbw, monzogranite of Bonanza King Wash; Jt, monzogranite of Tough Nut Spring; Jg, Jgg, Jgs, Jgqm, Jgm, Jgmr, Jgr, subunits of quartz monzonite of Goldstone; Jfr, Jfs, subunits of Fountain Peak Rhyolite. See full-scale map and Description of Map Units for details.

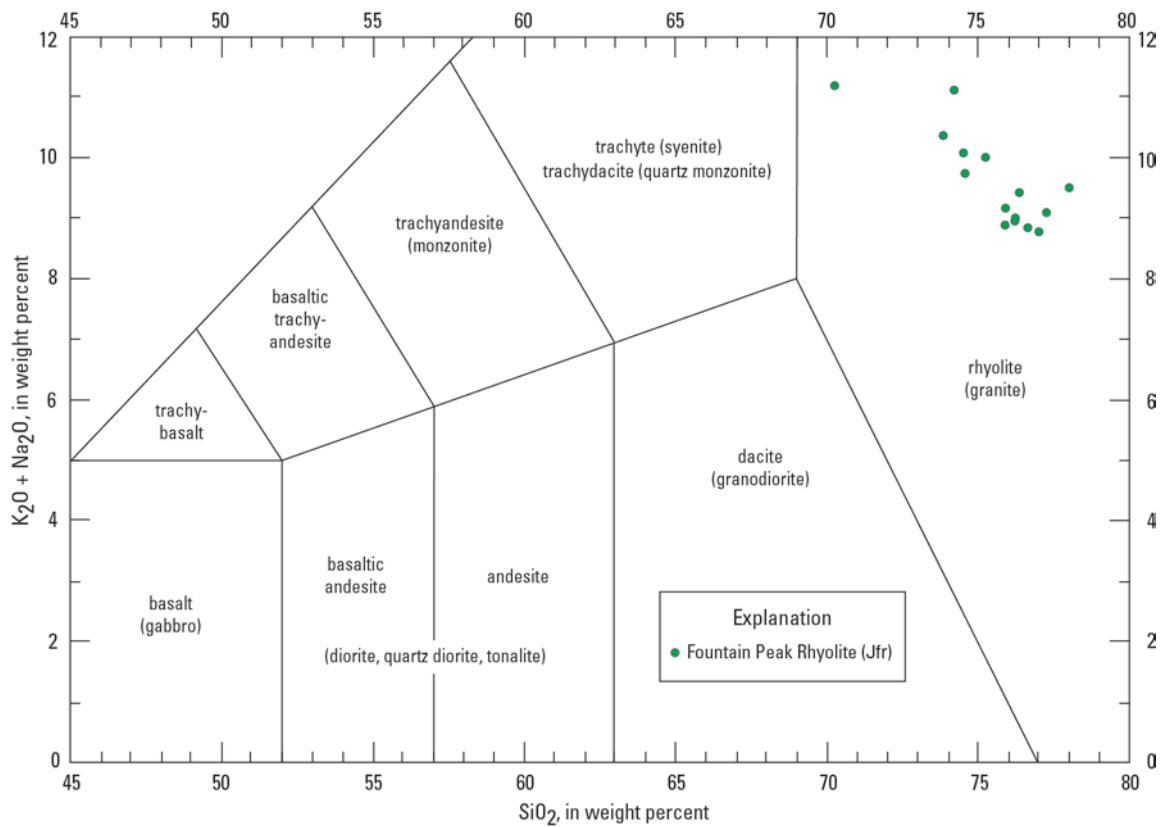


Figure 5. Total alkali-silica (TAS) plot showing geochemical composition of unit Jfr of Fountain Peak Rhyolite. Compositional fields from Best and Christiansen (2001) and LeMaitre and others (2002). Analytical data normalized to 100 percent (volatile-free). See appendix 3 for geochemical data.

Table 1. Summary of U-Pb zircon ages of selected Jurassic igneous rocks from the Providence Mountains in and near the Fountain Peak and adjacent 7.5' quadrangles, San Bernardino County, California.

[SHRIMP-RG (Sensitive High Resolution Ion MicroProbe-Reverse Geometry) ages determined in this study. See appendix 1 for sample localities and descriptions and appendix 4 for analytical data]

Sample number	Map unit label	Age (Ma)
Fountain Peak Rhyolite		
12-PR-3713	Jfr	163.6±1.4
12-PR-3889	Jfr	163.9±1.7
Plutonic rocks		
12-PR-3701	Jgqm	163.3±2.0
12-PR-3706	Jgm	167.8±1.8
13-PR-4854	Jbw	162.8±2.5
14-PR-5021	Jt	165.6±3.0
14-PR-5248	Jg	161.9±1.9
Dikes		
12-PR-3888	Jdf	162.4±1.1
14-PR-5023	Jdf	165.9±2.4

Contact relations of the Fountain Peak Rhyolite are variable. Along its northwest margin, massive rhyolite of unit **Jfr** intrudes the Pennsylvanian–Permian Bird Spring Formation (unit **PIPb**) and a thin sequence of volcanoclastic sedimentary rocks (unit **Jfs**) that disconformably overlies the Bird Spring (fig. 4). The contact is inferred to be faulted northwest of Edgar Peak, but an intrusive contact is again exposed to the northeast, wrapping around the strongly flow laminated northern prong of unit **Jfr** and cutting steeply across gently dipping strata of the Bird Spring Formation. This contact extends southward to a northeast-striking fault east of Fountain Peak. Southeast of that fault, a prominent unit of sandstone (unit **Jfs**) appears within the rhyolite body, and welded tuff textures are seen within the enclosing rhyolite of unit **Jfr**, indicating a surficial, non-intrusive mode of emplacement. The contact of unit **Jfr** with the Bird Spring Formation in this vicinity is therefore interpreted as depositional (fig. 4). Southward, this inferred depositional contact is obscured by faulting, but sedimentary and tuffaceous rocks of unit **Jfs** are discontinuously exposed within the rhyolite body. At its south margin, the Fountain Peak Rhyolite is apparently intruded by the Jurassic quartz monzonite of Goldstone (unit **Jg**; see next section). Finally, the southwest margin of the rhyolite body is faulted against the Bird Spring Formation and small sandstone outcrops of the Triassic Moenkopi Formation (unit **Tms**).

Based on lithologic characteristics and field relations (see Description of Map Units), the Fountain Peak Rhyolite is here interpreted as a rhyolite dome complex that intruded units as young as the oldest associated clastic rocks of unit **Jfs** and then spread out across the paleosurface, which was composed largely of Bird Spring Formation and minor overlying strata. Additional clastic sedimentation took place as the dome developed. The present outcrop area of the Fountain Peak Rhyolite is interpreted to represent only the intrusive conduit and the east half of the original dome (see cross section *B–B'*).

Jurassic Plutonic Rocks

Plutonic rocks that range in composition from gabbro to granite are present around the margins of the bedrock portion of the study area. Three first-order plutonic units are distinguished: the quartz monzonite of Goldstone, the monzogranite of Bonanza King Well, and the monzogranite of Tough Nut Spring (fig. 4). Geochronologic analyses during the present study (appendix 4) show that these units are late Middle to early Late Jurassic in age, confirming previous Jurassic age assignments based on regional correlations (Miller and others, 1985, 1991, 2007; Goldfarb and others, 1988). Geochemical analysis (fig. 6) indicates the large compositional range of the plutonic rocks.

The quartz monzonite of Goldstone crops out widely in the southern part of the map area and extends south beyond the area (Miller and others, 1985). This lithologically diverse plutonic suite is here divided into several units (fig. 4). The most extensive and heterogeneous unit (**Jg**) consists primarily of brown-weathering quartz monzonite and monzonite together with minor diorite, granodiorite, and syenite. These rocks are variably affected by albitic alteration (Fox and Miller, 1990) that commonly has bleached the rocks white and depleted them of potassium. Four subunits of more homogeneous lithology, mapped only west of Foshay Pass, consist of monzogranite (unit **Jgm**), quartz monzonite (unit **Jgqm**), fine-grained syenite to syenogranite (unit **Jgs**), and gabbro and diorite (unit **Jgg**). Another subunit (**Jgr**) west of Foshay Pass consists of reddish-brown granitic rocks that form narrow, north-trending bands and appear to be highly altered. Finally, a localized subunit (**Jgmr**) composed of red monzogranite forms four small outcrops east of Foshay Pass. Samples from units **Jgm**, **Jgqm**, and **Jg** yield U-Pb zircon ages of about 168, 163, and 162 Ma, respectively (table 1).

Contacts between the quartz monzonite of Goldstone and the adjacent Paleozoic rocks generally are faulted (fig. 4). The only definite intrusive contacts are near Foshay Pass and 0.8 km northeast of Blind Spring, where isolated outcrops of unit **Jg** poke through and clearly intrude the Bird Spring Formation (unit **PIPb**). Limestone and silty limestone of the Bird Spring Formation in these areas are widely metamorphosed to white marble and calc-silicate rock, consistent with an intrusive relation with unit **Jg**. Between the vicinities of Blind Spring and Foshay Spring, unit **Jg** is in contact with the

Fountain Peak Rhyolite (unit *Jfr*). Although detailed relations are obscured by poor exposure, the lateral continuity with the intrusive contacts to the west and east (fig. 4) suggests that unit *Jg* probably intrudes unit *Jfr* along this contact as well. This interpretation is consistent with geochronologic data suggesting that sample 14-PR-5248 from unit *Jg* is slightly younger than nearby sample 12-PR-3889 from unit *Jfr* (table 1; appendix 4).

The other two plutonic units are much less extensively exposed within the map area (fig. 4). The monzogranite of Bonanza King Well (unit *Jbw*) intrudes Paleoproterozoic gneiss and is overlain by Miocene volcanic rocks in the northeastern part of the area, east of the East Providence Fault of Hazzard (1954). This coarse-grained, relatively homogeneous granite yields a U-Pb zircon age of about 163 Ma (table 1). The monzogranite of Tough Nut Spring (unit *Jt*) intrudes Paleoproterozoic gneiss in the north-central part of the area and extends north beyond the area (Miller and others, 1991, 2007). This granite, much of which is highly altered, yields a U-Pb zircon age of about 166 Ma (table 1).

Jurassic Dikes

A large number of dikes (including a few irregular hypabyssal intrusive bodies) cut Jurassic and older rocks of the Providence Mountains. Aplite, felsic to intermediate, and diabase dikes are mapped separately; crosscutting relations suggest that the felsic to intermediate dikes are younger than the aplite dikes and older than the diabase dikes. All of the dikes are tentatively considered to be of Jurassic age although only two felsic dikes have actually been dated (table 1; appendix 4).

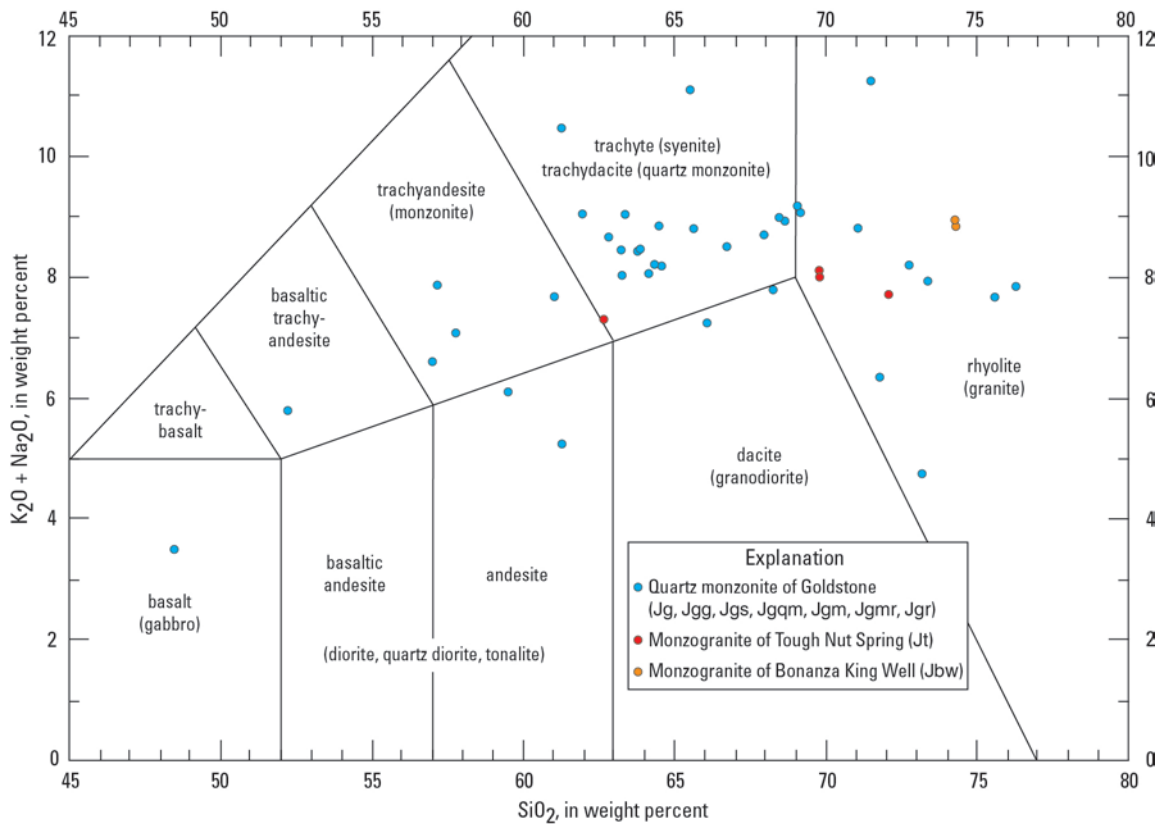


Figure 6. Total alkali-silica (TAS) plot showing geochemical compositions of plutonic rocks in map area. Compositional fields from Best and Christiansen (2001) and LeMaitre and others (2002). Analytical data normalized to 100 percent (volatile-free). See appendix 3 for geochemical data.

Mappable aplite dikes (unit **Jap**) are rare in the map area; only two such dikes that strike north to northeast and cut the quartz monzonite of Goldstone west of Foshay Pass were mapped. One of these is cut by a dike of felsic to intermediate composition.

The great majority of the dikes are of felsic to intermediate composition and are mapped as unit **Jdf**. Geochemical analysis indicates a range of compositions that include trachyandesite, trachydacite, trachyte, and rhyolite (fig. 7); most of the sampled dikes are rhyolite. Dikes of unit **Jdf** are most abundant in the southwestern and southeastern parts of the map area, where they cut the quartz monzonite of Goldstone and the Fountain Peak Rhyolite; in the northern part of the area, where they cut Paleozoic sedimentary rocks, the underlying Paleoproterozoic metamorphic rocks, and the monzogranite of Tough Nut Spring; and in the east-central part of the area, where they cut Pennsylvanian to Triassic sedimentary rocks near the margins of the Fountain Peak Rhyolite (unit **Jfr**). The latter dikes lithologically resemble rhyolite of unit **Jfr** and likely are genetically related to it. Dikes of unit **Jdf** dip steeply and many strike north to northwest. The dikes near the Fountain Peak Rhyolite, however, strike generally northeast, parallel to the northwest margin of the large rhyolite mass; some of these dikes intrude northeast-striking faults. Two dikes of unit **Jdf** yielded U-Pb zircon ages of about 162 and 166 Ma (table 1); both ages are identical within analytical error to the ages of the plutonic rocks they cut (appendix 4).

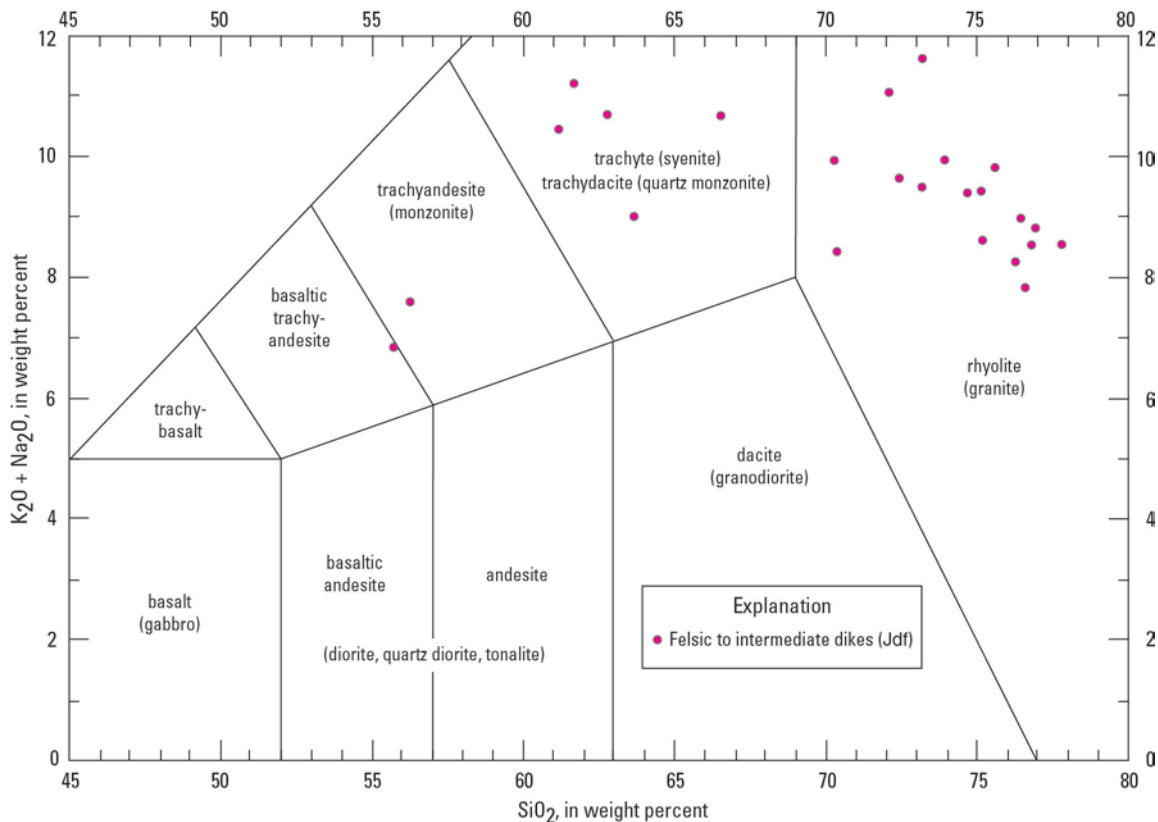


Figure 7. Total alkali-silica (TAS) plot showing geochemical compositions of felsic to intermediate dikes (unit **Jdf**) in map area. Compositional fields from Best and Christiansen (2001) and LeMaitre and others (2002). Analytical data normalized to 100 percent (volatile-free). See appendix 3 for geochemical data.

Diabase dikes (unit Jdd) are uncommon and were only observed cutting the Cambrian Chambless Limestone and Cadiz Formation. The two most prominent dikes, both of which cut the Cadiz Formation, strike generally east-west and dip south, nearly parallel to bedding in the host rock, and cut across the stratigraphic section at a low angle; technically these could be considered sills. One of these dikes, or sills, cuts a thick, north-striking dike of felsic to intermediate composition.

Age Relations of Jurassic Igneous Rocks

U-Pb zircon geochronology (table 1) indicates that all of the Jurassic igneous rocks in the study area were emplaced within a relatively short time interval between about 170 and 160 Ma. Moreover, a single statistical analysis of all of the zircon data combined produces a well constrained weighted mean age of about 164 Ma, with no discernible differences in age among the Jurassic plutons, the Fountain Peak Rhyolite (unit Jfr), and the felsic to intermediate Jurassic dikes (unit Jdf) (fig. 8). This close age similarity suggests that the plutons must have cooled very rapidly before being intruded by the associated dikes, a few of which also cut the Fountain Peak Rhyolite.

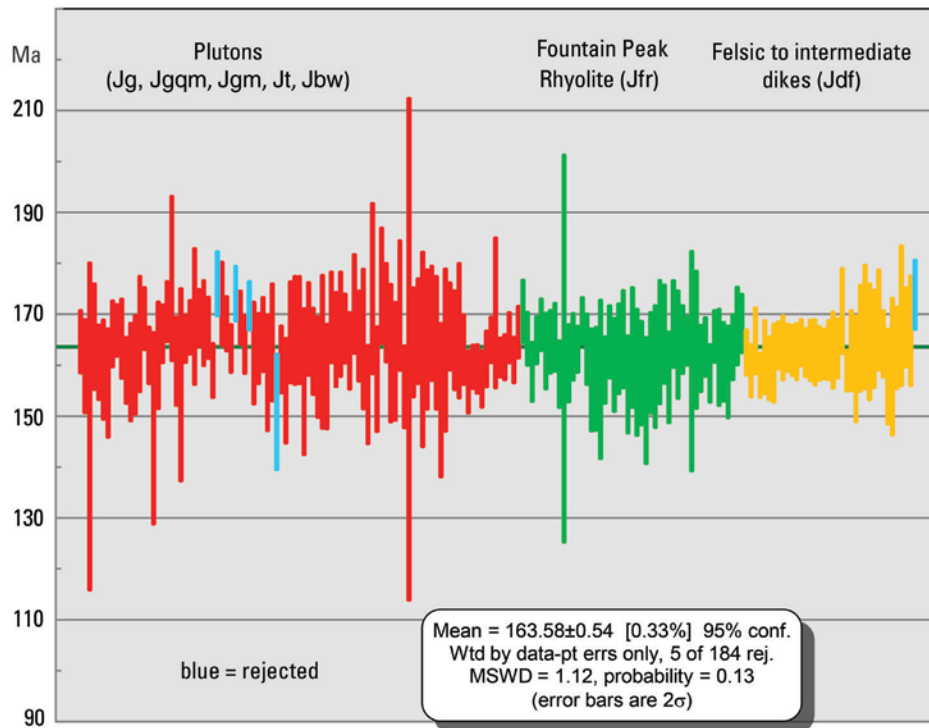


Figure 8. Weighted mean $^{206}\text{Pb}^*/^{238}\text{U}$ ages of individual zircon grains from analyzed Jurassic igneous rocks. For this diagram, data from plutons, Fountain Peak Rhyolite, and felsic to intermediate dikes were statistically analyzed together using Isoplot (Ludwig, 2008). Diagram shows that samples of all three rock types are of very similar age, with a mean of about 163.5 Ma. Bars depict 2-sigma errors; boxes show weighted mean crystallization ages, mean square weighted deviation (MSWD), and probability of fit. See appendix 4 for weighted mean ages of individual samples.

Miocene Volcanic Rocks

Pyroclastic volcanic rocks of Miocene age are exposed in several places along the east margin of the Providence Mountains. Correlative volcanic rocks that are much more extensively exposed north and east of the map area were mapped by McCurry (1985) and have been the subject of several additional topical studies (McCurry, 1988; Wells and Hillhouse, 1989; Buesch, 1991, 1993; McCurry and others, 1995).

Following previous usage, the oldest volcanic unit is here assigned to the regionally widespread Peach Spring Tuff (Billingsley and others, 1999), and all the younger rocks are assigned to the more localized Wild Horse Mesa Tuff of McCurry (1988). The Peach Spring Tuff consists of a single map unit (Tp), whereas the Wild Horse Mesa Tuff is here divided into five units (Tw1, Tw2w, Tw2u, Tw3, Tw4) that broadly correspond to members recognized by McCurry (1985, 1988). The Peach Spring Tuff and units Tw2w and Tw4 are cliff-forming, welded ash-flow tuffs; the other units include nonwelded ash-flow tuff and possible airfall tuff. Previous studies show that the ages of the Peach Spring Tuff and Wild Horse Mesa Tuff are about 18.8 Ma and 17.7–17.8 Ma, respectively (McCurry and others, 1995; Ferguson and others, 2013).

Whole-rock geochemical analysis shows that all of the Miocene volcanic units mapped during this study have a rhyolitic composition (fig. 9). The Peach Spring Tuff is distinguished by its relatively high titanium content (fig. 10), which is consistent with its characteristic abundance of sphene throughout its regional extent (Gusa and others, 1987).

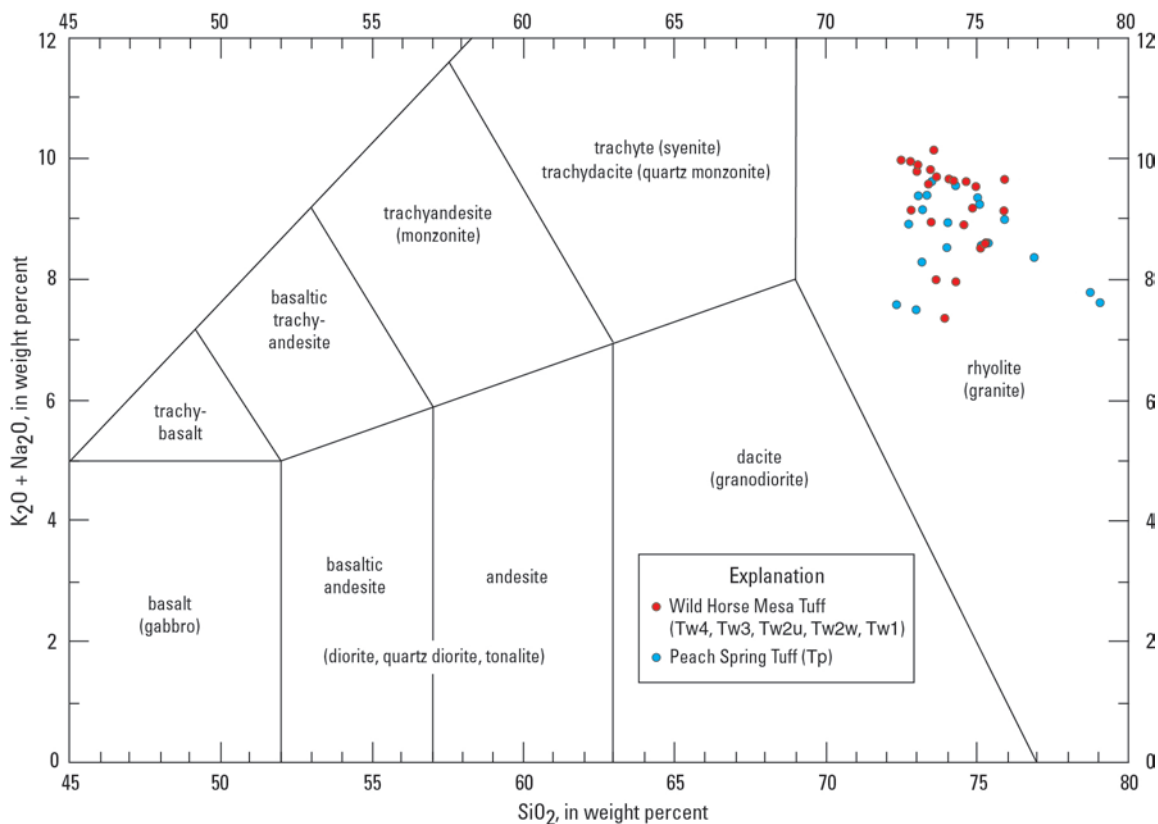


Figure 9. Total alkali-silica (TAS) plot showing geochemical compositions of Miocene volcanic rocks (Peach Spring Tuff and Wild Horse Mesa Tuff) in and near map area. Compositional fields from Best and Christiansen (2001) and LeMaitre and others (2002). Analytical data normalized to 100 percent (volatile-free). See appendix 3 for geochemical data.

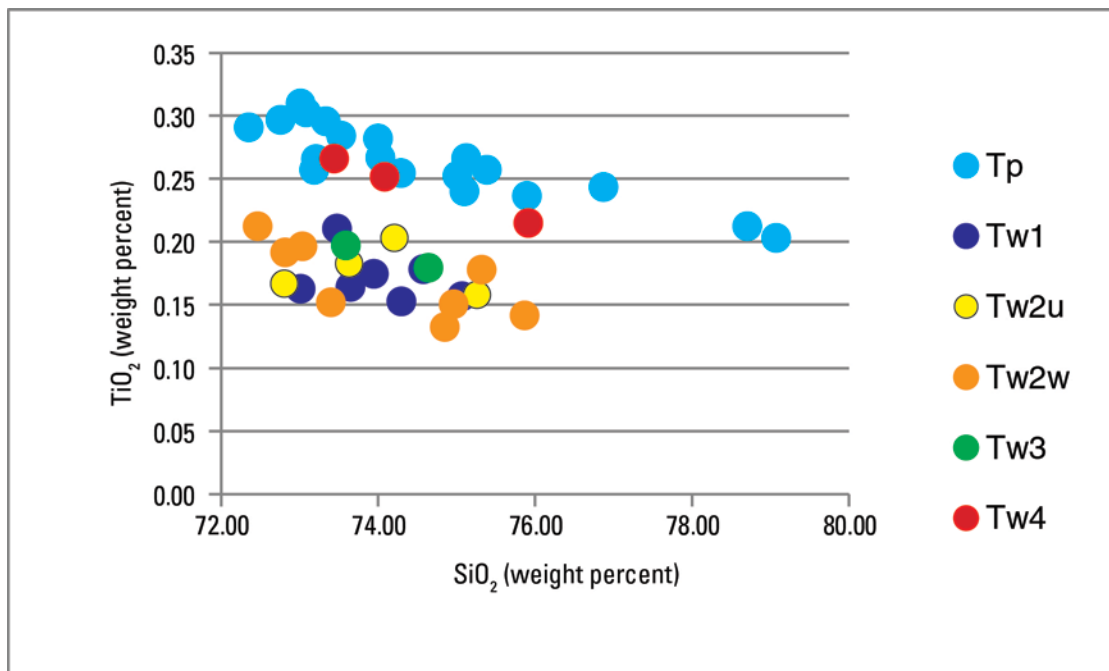


Figure 10. Harker diagram showing high titanium (TiO₂) vs. silica (SiO₂) content of Peach Spring Tuff (unit Tp) relative to that of most units of Wild Horse Mesa Tuff (units Tw1, Tw2u, Tw2w, Tw3). Titanium content of unit Tw4 is comparable to that of Peach Spring Tuff. Analytical data normalized to 100 percent (volatile-free). See appendix 3 for geochemical data.

The Miocene volcanic sequence rests nonconformably on Paleoproterozoic gneiss or Jurassic plutonic rocks and is confined to the area east of the East Providence Fault (fig. 4). All structurally higher pre-Miocene rocks (Neoproterozoic to Triassic sedimentary rocks and the Fountain Peak Rhyolite) that presumably had existed in this area were stripped away by erosional or tectonic processes prior to deposition of the Miocene volcanics.

Pliocene(?) and Quaternary Surficial Deposits

Various surficial deposits overlie Miocene and older rocks in the map area, extending out from slopes and canyons within the Providence Mountains to the marginal plains where broad alluvial fans developed. These deposits were not mapped or studied in great detail, although several units were differentiated. Most extensive are the alluvial deposits, which are divided into five units recognized primarily from surface morphologic features visible on aerial photographs (see Description of Map Units). These units (QToa, Qoa, Qia, Qya, Qaa) are based on the classification of Bedford and others (2010) with ages inferred from criteria such as those discussed by Bull (1991) and McDonald and others (1995). Two large landslide blocks of Pennsylvanian–Permian Bird Spring Formation (unit PIPb) and a mass of monolithologic breccia derived from tuff of the Fountain Peak Rhyolite (unit Jfs) were mapped within the oldest alluvial unit (QToa). Eolian sand (unit Qe), slope deposits (unit QTsl), and travertine and tufa (unit QTt) were also mapped. The slope deposits include talus, landslide debris, and colluvium.

Thin, lenticular beds of light-colored air-fall tuff (tephra) are interbedded with Pleistocene alluvium at four localities shown on the geologic map, and three of these were sampled for tephrochronologic analysis. One locality (sample 08-PR-1931) is in unit Qoa 1.85 km southeast of Rex Mine; the other three (including samples M08IV-1890 and 12-PR-3783) are several meters below a

desert pavement mapped as unit **Qia** in a deeply incised wash near the jeep road to Cornfield Spring. Tephrochronologic analyses (appendix 5) indicate that all three samples can be correlated with either the Bishop Tuff (~0.76 Ma) or the uppermost tuffs of Glass Mountain (~0.87 Ma) in the Long Valley Caldera area of east-central California (Sarna-Wojcicki and others, 2005), some 400 km northwest of the study area. These analyses are compatible with the work of McDonald and McFadden (1994), who previously correlated the same or similar tephra layers with the Bishop Tuff.

Structure

The geologic structure of the study area has been previously described and interpreted by Hazzard (1954), Miller and others (1985, 1996), and Goldfarb and others (1988). The present study supports most of the previous structural observations and interpretations, although a few structural features (mostly faults) shown here were not recognized during previous studies, and others are mapped slightly differently than by previous workers.

The dominant structural feature in the area is a southeast-dipping homocline formed by Neoproterozoic to Jurassic sedimentary rocks and the underlying Paleoproterozoic basement on the northwest side of the Providence Mountains (fig. 4; cross section *C–C'*). The dip of bedding in this homocline varies from about 20° to 60° and averages about 40°. The homocline is actually the western limb of a large, asymmetric syncline, the eastern limb of which is represented by west-dipping and locally overturned, west-facing beds on the east side of the range (cross section *B–B'*). The west-dipping beds include sandstone and tuff (unit **Jfs**) within the Jurassic Fountain Peak Rhyolite. This unit was evidently involved in the deformation that produced the syncline and its homoclinal western limb, although the subvertical, intrusive western margin of the unit does not appear to have been tilted.

The Paleoproterozoic to Jurassic sedimentary rocks and the Fountain Peak Rhyolite are cut by a complex network of faults, most of which have displacements of 100 m or less. The faults have a variety of orientations; most whose dips are known are normal faults, but a few exhibit reverse displacement. Faults of different orientation commonly merge with one another. Many of the faults are intruded by Jurassic dikes of felsic to intermediate composition (unit **Jdf**), but others cut such dikes. Particularly prominent faults (fig. 4) include (1) a group of west-dipping, moderate- to low-angle normal faults east of Rex Mine; (2) a group of east- to south-dipping, moderate-angle normal faults north and east of Vulcan Mine; and (3) a group of high-angle, northeast-striking faults near the range crest west of Edgar Peak. The normal faults of group 1 have a combined displacement of more than 2 km (cross section *B–B'*). Dikes commonly terminate against faults of groups 1 and 2, but may or may not be faulted; one fault in group 2 is clearly cut by a dike. One of the faults in group 2 appears to cut the Fountain Peak Rhyolite at its southwest end, but is apparently intruded by rhyolite at its northeast end (fig. 4). Faults of group 3 are intruded by several felsic dikes, some of which are lithologically similar to the Fountain Peak Rhyolite (unit **Jfr**).

Except along its margins, few faults appear to cut the Fountain Peak Rhyolite. The inferred fault with a curvilinear trace shown cutting the Fountain Peak Rhyolite from north to south (fig. 4) is based on lineaments seen on aerial photographs and local evidence of fault movement along contacts between units **Jfr** and **Jfs**. Based on the shape of its inferred trace and its apparent connection with a covered fault that offsets the contact between the Bird Spring and Moenkopi Formations to the north, this fault is interpreted as an east-dipping normal fault of modest displacement (cross section *B–B'*).

The two most significant faults in the study area are the Vulcan Mine and East Providence Faults (fig. 4), which bound the Paleozoic rocks on the southwest and east, respectively. Both faults dip steeply outward from the range but exhibit reverse displacement, with Jurassic plutonic rocks in the hanging wall of each and Paleoproterozoic metamorphic rocks in the hanging wall of the East Providence Fault (cross sections *A–A'* and *D–D'*). Thus, the topographically high Paleozoic rocks and Fountain Peak

Rhyolite occupy a relatively low structural position below the topographically lower rocks to the east and southwest.

The southwest-dipping Vulcan Mine Fault (fig. 4) places the quartz monzonite of Goldstone (mostly unit **Jgm**) above Cambrian to Devonian sedimentary rocks. Measured dips along the 2.5-km exposed length of the fault range from 70° to 83°. The dolomite-hosted iron ore body at Vulcan Mine is in the footwall of this fault. Northwest of Vulcan Mine, the footwall sedimentary rocks are locally folded, flattened, and slivered adjacent to the fault. Farther northwest, the Vulcan Mine Fault is inferred to continue in the subsurface and connect with a northwest-striking fault that cuts the quartz monzonite of Goldstone (unit **Jgqm**) at Rex Mine (fig. 4). A northeast-striking splay of the fault is inferred to lie buried between these plutonic rocks and the unmetamorphosed Cambrian rocks to the east. Southeastward, the Vulcan Mine Fault appears to terminate against an east-striking, high-angle fault that places quartz monzonite of Goldstone (unit **Jg**) against the Cambrian to Devonian dolomite (unit **Dcd**) that hosts the Vulcan Mine ore body. On the south side of this fault, 0.5 km to the west, a fault dipping 65° southwest within unit **Jg** may be the offset continuation of the Vulcan Mine Fault (fig. 4). This fault appears to terminate or die out about 1 km farther southeast.

The east-dipping East Providence Fault (Hazzard, 1954; Miller and others, 1996) is discontinuously exposed for a distance of about 9 km southward from the northern boundary of the map area (fig. 4). From north to south, the dip of the fault decreases from 75° to 60°, and progressively younger rocks are exposed in the footwall. In the northern part of the area, Cambrian to Devonian dolomitic rocks in the footwall are faulted against Paleoproterozoic metamorphic rocks (unit **Xm**). To the south, near C&K Mine (fig. 2), the Pennsylvanian–Permian Bird Spring Formation is faulted against the Paleoproterozoic rocks, which are intruded by Jurassic plutonic rocks assigned to the quartz monzonite of Goldstone (unit **Jg**) a short distance east of the fault (fig. 4). Still farther south, in the vicinity of Mitchell Caverns, Paleoproterozoic rocks are absent, and the Bird Spring Formation and the Jurassic Fountain Peak Rhyolite are faulted directly against unit **Jg**. Beyond its southernmost exposure, the buried fault is inferred to pass east of the southernmost outcrop of Bird Spring Formation, which caps an isolated hill of unit **Jg** (fig. 4).

The presence of Paleoproterozoic metamorphic rocks overlain by Miocene (~18–19 Ma) volcanic rocks in the hanging wall of the East Providence Fault indicates pre-volcanic, east-side-up displacement on the order of at least 2–3 km (Hazzard, 1954; Miller and others, 1996). As noted by these previous authors, this reverse fault movement could have been kinematically linked with development of the major syncline in the footwall. It is alternatively possible, however, that the fault could have functioned as a pre-synclinal, west-dipping normal fault that was later rotated to its present east dip when the synclinal folding took place (Miller and others, 1996).

East of Silver King Mine (fig. 2), a subvertical, northeast-striking fault with the southeast side down cuts Miocene volcanic rocks that overlie Paleoproterozoic metamorphic rocks (unit **Xm**) and the Jurassic monzogranite of Bonanza King Well (unit **Jbw**) (fig. 4). This fault, which has about 100 m of vertical displacement (cross section *D–D'*), is inferred to merge with the East Providence Fault between Silver King and Bonanza King Mines. This relation suggests that the East Providence Fault, at least south of the inferred fault junction, was reactivated as an east-side-down normal fault in Miocene or Pliocene time.

Few faults could be definitively traced through Jurassic plutonic rocks during this study, and those that were mapped cut various units of the quartz monzonite of Goldstone on the west side of the Providence Mountains. Most obvious is an east-dipping fault that separates a footwall of fine-grained syenite to syenogranite (unit **Jgs**) and a hanging wall of monzogranite (unit **Jgm**) and minor gabbro to diorite (unit **Jgg**) (fig. 4). The measured dip of this fault is 55°, but the sense of displacement is unknown. Beyond its exposed trace, this fault is inferred to terminate northward against the subsurface projection of the Vulcan Mine Fault and southward against the subsurface projection of the east-west

fault near Vulcan Mine (fig. 4). The other faults are in the area directly west of Foshay Pass. One of these, the possible offset equivalent of the Vulcan Mine Fault, has already been noted. The others are a related pair of apparent left-lateral strike-slip faults, one striking about N. 60° E. and the other east-west, that offset north- to northwest-striking bands of altered red granitic rocks (unit Jgr) about 300 and 100 m, respectively (fig. 4).

Faulting in the study area probably took place at several different times. At least one fault apparently is as old as Cambrian; this subvertical, north-striking fault in the northern part of the area appears to be depositionally overlapped by the distinctive siltstone marker unit (Ccs) of the Cadiz Formation 1.5 km southwest of Tough Nut Spring. Another fault, of apparent Devonian age in the western part of the area, is overlapped by beds in the Devonian limestone, dolomite, and quartzite unit (Dl) 1.5 km east of Rex Mine. Apart from these two examples, there is no direct evidence of significant faulting older than Triassic. Much of the faulting predated Jurassic emplacement of felsic to intermediate dikes (unit Jdf), and significant faulting also took place after emplacement of these dikes. The Vulcan Mine and East Providence Faults are clearly younger than about 163 Ma; Miller and others (1996) concluded that the East Providence Fault is latest Cretaceous based on relations north of the present study area. The youngest known faulting in the area offset the Miocene volcanic rocks near Silver King Mine and may have reactivated the East Providence Fault. No faults are known to cut the Quaternary deposits (Bedford and others, 2010).

Geologic History and Regional Relations

Paleoproterozoic basement rocks in the study area are part of the Mojave crustal province of Wooden and Miller (1990), the origins of which date back earlier than 2 Ga. Gneiss that forms the bulk of the basement complex in the study area formed about 1.71 Ga as a result of plutonism synchronous with a period of regional deformation and metamorphism known as the Ivanpah Orogeny. This orogeny took place midway through a major episode of plutonism that lasted from 1.76 to 1.64 Ga.

Sedimentation on the eroded remnants of the Paleoproterozoic basement complex began in late Neoproterozoic (Ediacaran) time with deposition of the Johnnie Formation between about 630 and 540 Ma (Bergmann and others, 2011). Neoproterozoic to Early Triassic sedimentary rocks in the study area are of cratonal to miogeoclinal affinity and represent deposition on the inner part of a northeast-trending, northwest-facing continental shelf that originated on a passive, rifted continental margin (Burchfiel and Davis, 1981; Dickinson, 1981). Continent-derived siliciclastic sedimentation characterized the shelf through the Early Cambrian and was replaced by carbonate and minor siliciclastic sedimentation that began in the Middle Cambrian and continued through the remainder of the Paleozoic. Lithologic and faunal characteristics indicate shallow-water conditions throughout this time; differences between successive units reflect fluctuations in such factors as water depth, temperature, and chemistry through time. Following deposition of the Bird Spring Formation in the Early Permian, the shelf became emergent and subject to erosion (Stone and others, 2013). By the Early Triassic the shelf was again submerged and received an influx of fine-grained continental siliciclastic detritus followed by a final episode of carbonate sedimentation recorded by the Moenkopi Formation.

Erosion of the Moenkopi and Bird Spring Formations in later Triassic or Jurassic time produced a thin conglomerate. This sedimentation was followed by an intense and widespread episode of late Early to early Late Jurassic (~170–160 Ma) magmatic activity that included emplacement of a rhyolite dome complex (Fountain Peak Rhyolite), deposition of spatially related volcaniclastic sandstone, and the intrusion of several plutons and numerous dikes. Volcanic and plutonic rocks of approximately the same age are abundant throughout the Mojave Desert region (Haxel and Miller, 2007) and were part of an extensive Andean-type arc that formed above an east-dipping subduction zone along the North American continental margin (Hamilton, 1969; Burchfiel and Davis, 1975; Busby-Spera, 1988).

Faulting took place in the study area before, after, and possibly during the Jurassic magmatic episode, fragmenting the crust into numerous structural blocks. The exact age and regional significance of most faults in the area are unknown, including the prominent low- to moderate-angle normal fault zone exposed on the northwest side of the Providence Mountains. Despite the presence of a few reverse faults, the study area apparently was unaffected by regional, large-scale, east-directed Mesozoic thrust faulting and associated folding that have been documented in ranges to the north and northeast including the Clark Mountain Range, Ivanpah Mountains, and New York Mountains (Burchfiel and Davis, 1981).

The most significant fault in the study area, the East Providence Fault, has been interpreted as part of a composite, Late Cretaceous fault zone (East Mojave Fault) that can be traced some 70 km northward from the southern Providence Mountains to an area northwest of Cima (Miller and others, 1996). Those authors and later Wells and others (2005) suggested that this composite fault could have been part of an even more extensive fault system that connected areas of major Late Cretaceous crustal extension to the north and south. Geometrically similar, north- to northwest-striking, high-angle faults of late Mesozoic age that juxtapose Paleozoic rocks on the west against Precambrian basement rocks on the east are present to the northwest at Old Dad Mountain (Prospect Shear Zone of Dunne, 1977) and to the north and northeast in the Clark Mountain Range and New York Mountains (Kokoweef-Slaughterhouse composite fault of Burchfiel and Davis, 1977). Both of these other fault zones show evidence of possible strike-slip movement, and it is possible that the East Providence Fault had an early history of strike-slip movement as well (Miller and others, 1996).

Widespread late Cenozoic volcanism in the Mojave Desert and adjoining regions (Sherrod and Nielson, 1993) included the Early Miocene emplacement of the ~18.8 Ma Peach Spring Tuff and the ~17.7–17.8 Ma Wild Horse Mesa Tuff in the eastern part of the study area. The Peach Spring Tuff was erupted from the Silver Creek Caldera of Ferguson and others (2013) 100 km to the east, whereas the Wild Horse Mesa Tuff was erupted from the Woods Mountains Volcanic Center of McCurry (1985, 1988) just 20 km to the east. Both tuff units are confined to the area east of the East Providence Fault (McCurry, 1985), but it is unclear whether these tuffs predate or postdate this fault. It is possible that the tuffs originally abutted against a pre-existing fault or fault-line scarp and were later cut when the fault was reactivated. McCurry and others (1995) presented evidence that the Providence Mountains north of the study area were relatively subdued topographically at the time the tuffs were emplaced and were later uplifted 300 to 500 m owing to a combination of faulting and tilting.

Since the time of the latest known faulting, which postdated emplacement of the Wild Horse Mesa Tuff, uplands in the study area have been deeply eroded and the surrounding valleys filled with alluvial and other surficial deposits (Bedford and others, 2010; Miller, 2012). The absence of exposed Quaternary faults and the relatively shallow depths to basement beneath the valleys (Langenheim and others, 2009) are consistent with the interpretation that periods of alluvial-fan deposition adjacent to the Providence Mountains have likely been controlled mainly by regional climate changes rather than tectonics (McDonald and McFadden, 1994; McDonald and others, 1995).

DESCRIPTION OF MAP UNITS

[Names and ages of Neoproterozoic to Triassic units are from Hazzard (1954) with modifications as explained. Mineral compositions of igneous rocks are estimated from stained and unstained slabs and thin sections (appendix 1, table 2). Chemical data (oxide concentrations; appendix 3, table 4) are from whole-rock X-ray fluorescence (XRF) analyses contracted by USGS and are reported as volatile-free weight percent. Classification of igneous rocks is based in part on total alkali-silica (TAS) plots of $K_2O + Na_2O$ vs. SiO_2 (figs. 5–7; Best and Christiansen, 2001; LeMaitre and others, 2002). Uranium-lead (U-Pb) zircon ages of igneous rocks (appendix 4, table 6, figs. 17–19) are from analyses carried out on the U.S. Geological Survey (USGS) SHRIMP-RG (Sensitive High Resolution Ion MicroProbe–Reverse Geometry) ion microprobe at Stanford University]

- ml **Modified land (Holocene)**—Land surface significantly altered by pipeline and road construction in southern part of map area
- mw **Mine waste (Holocene)**—Accumulations of rock waste produced by mining activities (Vulcan and Bonanza King Mines)
- Qe **Eolian sand (Quaternary)**—Small eolian sand dunes in southwestern part of map area
- QTs **Slope deposits, undivided (Quaternary and Pliocene?)**—Diverse deposits of unconsolidated to loosely consolidated rock material on slopes, including colluvium, talus, and landslide debris
- QTt **Travertine and tufa (Quaternary and (or) Pliocene?)**—White to cream-colored deposits of calcium carbonate inferred to mark former locations of groundwater discharge. Includes two small deposits along a strike-slip fault in southern part of map area
- Alluvial deposits (Holocene to Pliocene?)**—Poorly to moderately sorted sand and gravel deposited by stream activity in alluvial fans and washes. Divided into five subunits based primarily on surface characteristics and morphologic relations as interpreted from aerial photographs; detailed field study of these deposits and their soils was not conducted. Age assignments are from Bedford and others (2010)
- Qaa **Active and recently active alluvial deposits (Holocene)**—Deposits largely confined to modern washes, ranging from very recent deposits composed of loose sand and gravel to relatively old, weakly consolidated terrace deposits, some of which may overlap in age with unit Qya. Surfaces typically appear gray to brown on aerial photographs. Equivalent to unit Q4 of Bull (1991)
- Qya **Young alluvial deposits (Holocene and latest Pleistocene)**—Weakly consolidated sand and gravel forming surfaces incised by unit Qaa. Surfaces are characterized by relict bar and swale morphology and weakly developed desert varnish; typically appear medium-brown on aerial photographs. Equivalent to unit Q3 of Bull (1991)
- Qia **Intermediate alluvial deposits (late to middle Pleistocene)**—Moderately consolidated sand and gravel forming surfaces incised by units Qya and Qaa. Surfaces are drained by dendritic networks of shallow channels and are characterized by well-developed desert pavement and desert varnish; typically appear dark brown on aerial photographs. Equivalent to unit Q2 of Bull (1991)

- Qoa** **Old alluvial deposits (middle to early Pleistocene)**—Well-consolidated sand and gravel forming surfaces incised by unit **Qia** and younger deposits. Surfaces are deeply dissected into ridges and ravines and generally have no desert varnish; typically appear very light brown on aerial photographs. Many ridges are capped by layers solidly cemented by caliche. Together with unit **QToa**, equivalent to unit **Q1** of Bull (1991)
- QToa** **Extremely old alluvial deposits (early Pleistocene to Pliocene?)**—Well-consolidated sand and gravel forming surfaces incised by unit **Qoa** and younger deposits. Similar in morphology to unit **Qoa** but topographically higher and more deeply dissected
- Wild Horse Mesa Tuff (Miocene)**—Sequence of rhyolitic tuffs exposed on east flank of Providence Mountains; interpreted to have been erupted from the Miocene Woods Mountains Volcanic Center ~15 km east-northeast of map area (McCurry, 1985, 1988; McCurry and others, 1995; Miller and others, 2007). $^{40}\text{Ar}/^{39}\text{Ar}$ age of 17.8–17.7 Ma was reported by McCurry and others (1995), but without supporting data. Maximum reported thickness of tuff sequence is 320 m at Wild Horse Mesa, about 7 km east-northeast of map area (McCurry, 1988); maximum partial thickness on hill 1432T northeast of Silver King Mine is ~220 m
- Tw4** **Unit 4**—Cliff-forming ash-flow tuff that forms summit of hill 1432T; top eroded; consists of upper, middle, and lower subunits about 8, 2, and 10 m thick, respectively. Upper subunit is a distinctive, dark-brown-weathering welded tuff characterized by abundant lenticular, crystallized pumice clasts and weathering pits mostly ≤ 2 cm long; a fine-grained, crystalline groundmass encloses scattered sanidine crystals ~1 mm long. Middle subunit consists of dense, dark-gray welded tuff containing sparse sanidine crystals ≤ 1 mm long and abundant small, highly flattened feldspar clasts in a fine-grained crystalline groundmass with relict vitroclastic texture. Lower subunit consists of 10 m of light-brownish-gray welded tuff that contains elongate, dark-brown pumice fragments ≤ 2 cm long, light-gray lithic fragments ≤ 3 mm long, and scattered sanidine crystals. Contacts between subunits are gradational. Samples from each subunit are chemically similar, containing ~73.5–76 percent SiO_2 , 9.6–9.8 percent $\text{K}_2\text{O} + \text{Na}_2\text{O}$, and a higher titanium content (0.21–0.27 percent TiO_2) relative to SiO_2 than underlying units of the Wild Horse Mesa Tuff. Unit is equivalent to lower part of the upper member of the Wild Horse Mesa Tuff of McCurry (1988). Total exposed thickness ~20 m
- Tw3** **Unit 3**—Light-gray, massive, weakly consolidated, unwelded tuff characterized by large-scale cavernous weathering; forms slope between cliff-forming welded tuffs of units **Tw2w** and **Tw4**. Tuff contains abundant light-brown to purplish-gray, unflattened, crystallized pumice clasts ≤ 2.5 cm long in a fine-grained, crystalline groundmass that retains no relict vitroclastic texture; scattered sanidine crystals ≤ 2 mm long; rare biotite; and rare large crystals (4 mm) of microcline presumably reworked from granitic bedrock. Sanidine crystals are present in some pumice clasts. Strongly lithified, spherical to ovoid concretions of similar composition to host rock are locally abundant near base of unit. A representative sample of unit contains ~73.5 percent SiO_2 , 10.1 percent $\text{K}_2\text{O} + \text{Na}_2\text{O}$, and 0.20 percent TiO_2 . Unit is equivalent to upper

part of the middle member of the Wild Horse Mesa Tuff of McCurry (1985).
Thickness ~60 m

Unit 2—Ash-flow tuff equivalent to lower part of the middle member of the Wild Horse Mesa Tuff of McCurry (1985); includes a welded and an unwelded facies. In outcrops ~1 km southeast of Bonanza King Mine, the unwelded facies (unit Tw2u) overlies the welded facies (unit Tw2w); to the north and south, unit consists entirely of the welded and unwelded facies, respectively. The two facies are interpreted to be closely related based on their similar lithologic and chemical compositions. Maximum thickness in map area is ~100 m

Tw2u

Unwelded facies—Light-brown to light-pinkish-brown, massive, low-density tuff characterized by abundant reddish-brown pumice fragments mostly ≤ 1 cm long. Pumice fragments are mostly oblong but do not appear to be highly flattened. As seen in thin section, both the pumice fragments and the enclosing groundmass are isotropic (glassy); the groundmass displays an unwelded vitroclastic texture with well-preserved shards. Including pumice fragments, sand-size and larger clasts typically make up ~30–40 percent of the rock volume; clasts include free crystals (mostly sanidine), felsic volcanic rock fragments, and rare granitic rock fragments. Four samples contain ~73–75 percent SiO₂, 8.6–9.7 percent K₂O + Na₂O, and 0.16–0.20 percent TiO₂

Tw2w

Welded facies—Pink to brown, strongly lithified, cliff-forming, welded tuff containing 30–50 percent sand-size and larger clasts floating in a fine-grained groundmass. Clasts include pumice fragments, crystals, and rare lithoclasts. Pumice fragments are elongate, dark brown to purplish brown, and ≤ 3 cm long and 1 cm thick; most are flattened and aligned with stratification. The pumice fragments are crystallized and some are spherulitic. Crystals are almost all anhedral to subhedral sanidine ≤ 2 mm in diameter; biotite and plagioclase crystals are rare. Some plagioclase crystals are sericitized and probably were reworked from older rocks. Lithoclasts are mostly fine-grained volcanic(?) rocks; one granitic rock fragment containing microcline was observed. The glassy to finely crystalline groundmass contains crystallized shards and small pumice fragments that are strongly flattened and commonly bent around adjacent crystals. Base of unit is marked by a distinctive, light-yellowish-brown, unwelded to weakly welded tuff that has well-developed columnar jointing and forms a continuous ledge about 2 m high; this rock contains 30–40 percent sand-size and larger clasts including orange pumice fragments as much as 7 mm long, felsic volcanic and minor fine-grained granitic lithoclasts as much as 4 mm long, and sanidine crystals in a glassy groundmass containing abundant yellowish-brown, crystallized shards. Eight samples of unit, including the basal yellow tuff, contain ~72.5–76 percent SiO₂, 8.6–10 percent K₂O + Na₂O, and 0.13–0.20 percent TiO₂

Tw1

Unit 1—White to light-gray, weakly to moderately consolidated, massive to weakly laminated tuff that typically forms recessive slopes but locally forms bold outcrops. Tuff is vitroclastic and unwelded, composed primarily of well-preserved, randomly oriented glass shards and glassy pumice fragments ≤ 1 cm long; sanidine and rare plagioclase crystals form ≤ 5 percent of the rock. Pumice clasts have form ratios $\leq 3:1$ but do not appear to be significantly flattened. In many places, the tuff also contains abundant volcanic and granitic

lithoclasts ≤ 4 cm long; the dominant clasts in one sample are glassy to felsitic volcanic rocks, some of which contain well-preserved shards that strongly suggest a Cenozoic source-rock age. Seven samples contain ~ 73 – 75 percent SiO_2 , 7.4 – 9.8 percent $\text{K}_2\text{O} + \text{Na}_2\text{O}$, and 0.15 – 0.21 percent TiO_2 . Maximum thickness ~ 40 m

- Tp Peach Spring Tuff (Miocene)**—Light-gray to pinkish-gray, purplish-gray, and pink, cliff-forming ash-flow tuff correlated with the regionally extensive Peach Spring Tuff of Young (*in* Billingsley and others, 1999; formerly Peach Springs Tuff of Young and Brennan, 1974). Unit forms small, isolated outcrops in map area but is more continuously exposed in adjacent areas to the north and east (McCurry, 1985, 1988; Wells and Hillhouse, 1989; Buesch, 1991; Miller and others, 2007). In map area, unit primarily consists of welded tuff that contains elongate brown, crystallized pumice fragments ≤ 3 cm long and ~ 20 percent crystals ≤ 3 mm long (abundant sanidine, subordinate plagioclase and biotite, and rare but conspicuous sphene); the groundmass varies from glassy to felsitic and commonly has a well-preserved to relict vitroclastic texture with welded and compacted shards. Parts of unit show less evidence of welding and compaction. Nineteen samples contain ~ 72 – 79 percent SiO_2 , 7.6 – 9.6 percent $\text{K}_2\text{O} + \text{Na}_2\text{O}$, and 0.20 – 0.30 percent TiO_2 ; the relatively high titanium content relative to SiO_2 helps distinguish this unit from units 1–3 of the Wild Horse Mesa Tuff. Undated in map area; regional age is ~ 18.8 Ma (Ferguson and others, 2013). Maximum exposed thickness in map area is ~ 60 m
- Jdd Diabase dikes (Jurassic?)**—Fine-grained diabase dikes 2 to 5 m thick that cut Cambrian rocks in northern part of map area, particularly the Cadiz Formation. Dikes strike easterly, approximately parallel to the strike of the host rocks. One dike cuts a felsic dike of unit Jdf. Undated
- Jdf Felsic to intermediate dikes (Jurassic)**—Dikes of diverse composition and lithology that cut rocks of Jurassic and older age. Most mapped dikes are 5 to 20 m thick, 0.2 to 3 km long, and strike northwest to northeast; many unmapped, smaller dikes are also present. Dike rocks are variably light to dark shades of gray, brown, brownish gray, greenish gray, red, reddish gray, and reddish brown in color. Most dikes are porphyritic, containing 5–30 percent euhedral to subhedral phenocrysts of plagioclase and potassium feldspar 2–10 mm long in a fine-grained crystalline groundmass; some of the more felsic dikes also contain subequant quartz phenocrysts < 1 – 4 mm in diameter. Mafic phenocrysts, primarily biotite, are uncommon to rare. Chemical composition of 24 samples varies from rhyolite (17 samples, ~ 70 – 78 percent SiO_2 and ~ 8 – 12 percent $\text{K}_2\text{O} + \text{Na}_2\text{O}$) to trachyte and (or) trachydacite (5 samples, ~ 61 – 66 percent SiO_2 and ~ 9 – 11 percent $\text{K}_2\text{O} + \text{Na}_2\text{O}$) to trachyandesite and basaltic trachyandesite (2 samples, ~ 56 percent SiO_2 and ~ 7 – 8 percent $\text{K}_2\text{O} + \text{Na}_2\text{O}$). The most silicic dikes are chemically similar to rhyolite of unit Jfr; dikes near the margins of unit Jfr probably are genetically related to that unit. The most mafic, dark-colored dikes are either uniformly fine-grained or contain scattered phenocrysts of light-red plagioclase; many small, unmapped dikes of this type cut Jurassic plutonic rocks (unit Jg) in southern part of map area. Unit age is interpreted as late Middle to early Late Jurassic based on U-Pb zircon ages of 162.4 ± 1.1 Ma for a red rhyolite dike (sample 12-PR-3888) that

- cuts the quartz monzonite of Goldstone (unit **Jg**) and the Fountain Peak Rhyolite (unit **Jfr**) in southeastern part of map area and 165.9 ± 2.4 Ma for a light-pinkish-gray rhyolite dike (sample 14-PR-5023) that cuts the monzogranite of Tough Nut Spring (unit **Jt**) a short distance north of map area
- Jap** **Aplite dikes (Jurassic)**—White, medium-grained aplite dikes as much as 10 m thick that cut Jurassic granitoid rocks (units **Jg**, **Jgm**) and are cut by younger Jurassic dikes (unit **Jdf**). The two mapped dikes strike northerly to northeasterly
- Jbw** **Monzogranite of Bonanza King Well (Jurassic)**—Light-gray to yellowish-brown, coarse-grained, equigranular monzogranite in northeastern part of map area; intrudes Paleoproterozoic gneiss (unit **Xm**). Highly fractured; commonly weathered to grus. Composed of subequal amounts of potassium feldspar (red, poikilitic), plagioclase (white, variably sericitized), and quartz, with only 1–2 percent dark minerals, most of which are iron oxides. Average grain size ~5 mm; potassium feldspar crystals are as much as ~1 cm long. Two representative samples contain ~74 percent SiO_2 and ~9 percent $\text{K}_2\text{O} + \text{Na}_2\text{O}$. In places, granite is cut by unmapped quartz-rich veins or dikes. Sample 13-PR-4854 yielded a late Middle to early Late Jurassic U-Pb zircon age of 162.8 ± 2.5 Ma
- Jt** **Monzogranite of Tough Nut Spring (Jurassic)**—Equigranular to porphyritic, medium- to coarse-grained monzogranite in north-central part of map area; intrudes Paleoproterozoic gneiss (unit **Xm**). Unweathered outcrops, present mainly in wash bottoms, are light to medium gray; outcrops on hills and slopes typically are subdued and weathered reddish brown. Composed of subequal amounts of potassium feldspar (pink, red, and reddish gray), plagioclase (white, partly to almost completely sericitized), and quartz, 5–10 percent biotite (partly replaced by chlorite), and <5 percent iron oxides; potassium feldspar commonly forms phenocrysts <1 to 2 cm long. Average grain size, excluding phenocrysts, is ~3 mm. Two representative samples from fresh outcrops contain ~70 percent SiO_2 and ~8 percent $\text{K}_2\text{O} + \text{Na}_2\text{O}$; weathered samples are of more varied chemical composition. Sample 14-PR-5021 just north of quadrangle boundary yielded a late Middle to early Late Jurassic U-Pb zircon age of 165.6 ± 3.0 Ma
- Quartz monzonite of Goldstone (Jurassic)**—Lithologically diverse plutonic rocks exposed in southern part of map area (Miller and others, 1985, 2007; Goldfarb and others, 1988; Fox and Miller, 1990). Rocks of this plutonic suite are primarily quartz monzonite and monzonite but also include gabbro, diorite, syenite, and granite; these rocks are here divided into seven map units. In most places, the rocks are faulted against Paleozoic sedimentary rocks; locally, however, monzonite or quartz monzonite of unit **Jg** intrudes the Bird Spring Formation and is interpreted to intrude the Fountain Peak Rhyolite as well. Age of the plutonic suite is based on regional relations (Miller and others, 1985) and on late Middle to early Late Jurassic U-Pb zircon ages of 161.9 ± 1.9 Ma for monzonite (unit **Jg**, sample 14-PR-5248), 163.3 ± 2.0 Ma for quartz monzonite (unit **Jgqm**, sample 12-PR-3701), and 167.8 ± 1.8 Ma for monzogranite (unit **Jgm**, sample 12-PR-3706)
- Jg** **Undivided rocks**—Primarily quartz monzonite and monzonite characterized by extensive sodium metasomatism (albitization) (Fox and Miller, 1990). Rocks

are mostly medium grained (average grain size 2–3 mm), equigranular to weakly porphyritic, and range from weakly altered to completely albitized. Unweathered, weakly altered rocks typically are pinkish gray and consist of 25–35 percent each of pink to reddish-gray potassium feldspar and white to light-greenish-gray plagioclase, 5–15 percent quartz, 15–30 percent mafic minerals (hornblende > biotite > pyroxene), and 1–5 percent iron oxides. Plagioclase is weakly to strongly sericitized and commonly forms euhedral to subhedral phenocrysts 4–6 mm long; mafic minerals are partially replaced by chlorite in most samples but generally retain a dark color. Outcrops range from bold and resistant to highly weathered and recessive; weathered outcrops typically are dark brown with small white spots formed by plagioclase phenocrysts. Strongly to completely albitized rocks, by contrast, are white to light gray due to depletion of potassium feldspar and intense bleaching and alteration of the mafic minerals. In many samples, stained slabs and thin sections show that all the feldspar in these altered rocks is plagioclase, much of which is presumably albite formed by alteration of potassium feldspar. Chlorite and epidote are common, presumably as replacements of mafic minerals. The albitized rocks form resistant outcrops that range from large, irregular masses with indistinct boundaries to small dikes that cut sharply across less altered rocks.

Chemically, 17 samples of weakly to completely altered rocks from this unit contain ~57–67 percent SiO₂ and ~5–10 percent K₂O + Na₂O; all but two of these have ~6–9 percent K₂O + Na₂O. On this basis, most of the rocks are classified as quartz monzonite and monzonite; a few are diorite, granodiorite, and syenite. Granite probably also is present in small amounts, although none was chemically analyzed. Chemical analysis also shows that the albitized rocks are enriched in sodium (>4.7 percent Na₂O) and depleted in potassium (<1.5 percent K₂O) as a result of metasomatism

- Jgg** **Gabbro and diorite**—Dark-gray, fine- to coarse-grained, equigranular plutonic rocks composed of subequal plagioclase and mafic minerals that include biotite, hornblende, and pyroxene(?). One representative sample of medium-grained gabbro contains ~48.5 percent SiO₂ and ~3.5 percent total alkalis. Forms relatively small outcrop areas adjacent to less mafic rocks of units **Jg** and **Jgm**; relative age relations with these units are unclear from field observations. Commonly cut by light-colored dikes or dike-like bodies that probably are zones of albitic alteration
- Jgs** **Fine-grained syenite to syenogranite**—Light-gray, light-purplish-gray, and light-red, fine-grained rocks west of Vulcan Mine. Equigranular to porphyritic; groundmass is microcrystalline to fine-grained felsite composed of potassium feldspar, plagioclase, and minor quartz; phenocrysts of potassium feldspar and plagioclase mostly 1–7 mm long form as much as 30 percent of the rock volume. Stained slabs and thin sections show that potassium feldspar is significantly more abundant than plagioclase, both in the groundmass and as phenocrysts. Scattered biotite crystals ≤2 mm long typically form 1–2 percent of the rock volume. Two representative samples contain ~65–71 percent SiO₂ and ~11 percent K₂O + Na₂O. Undated; Jurassic age inferred although relative age relation to adjacent quartz monzonite (unit

- Jgqm) is unclear from field observations. Faulted against monzogranite (unit Jgm) and gabbro/diorite (unit Jgg)
- Jgqm** **Quartz monzonite**—Reddish-gray, medium-grained, equigranular to weakly porphyritic quartz monzonite west of Vulcan Mine. Typically composed of 35–40 percent red potassium feldspar, 30–40 percent white plagioclase, 5–20 percent quartz, and 5–20 percent mafic minerals including iron oxides; a few samples have as much as 40 percent mafic minerals. Average grain size 2–3 mm. Plagioclase, which is strongly sericitized, commonly forms anhedral to euhedral phenocrysts as much as 6 mm long; mafic minerals are biotite and subordinate hornblende. No albitic alteration noted. Unit is characterized by its distinctive rock color, which is largely due to the abundance of unaltered red potassium feldspar. Four typical samples have ~63–64 percent SiO₂ and ~8.5–9 percent K₂O + Na₂O; one unusually mafic sample has ~52 percent SiO₂ and ~5.8 percent K₂O + Na₂O
- Jgm** **Monzogranite**—Light-gray to light-reddish-gray, medium-grained, equigranular to porphyritic monzogranite west and south of Vulcan Mine. Most rocks are unaltered to weakly altered, but some are strongly to completely albitized. Unaltered to weakly altered rocks are composed of 30–45 percent potassium feldspar (commonly pink to reddish gray), 20–45 percent plagioclase (white to light greenish gray, some highly sericitized), 20–30 percent quartz, and <5–10 percent biotite that is commonly replaced by chlorite; many samples contain subequal amounts of potassium feldspar, plagioclase, and quartz. Average grain size in equigranular rocks is 2–4 mm. Porphyritic rocks typically contain as much as 30 percent red potassium feldspar phenocrysts 5–20 mm long; some samples contain plagioclase phenocrysts generally ≤5 mm long. By contrast, strongly to completely albitized rocks typically are composed of 60–70 percent plagioclase, 20–30 percent quartz, and 5–10 percent altered biotite or chlorite. Eight representative samples of unit have ~68–76 percent SiO₂ and ~7.5–9 percent K₂O + Na₂O; of these, one strongly albitized sample is enriched in sodium (7.4 percent Na₂O) and depleted in potassium (0.8 percent K₂O) as a result of metasomatism. Contact with undivided rocks of unit Jg south of Vulcan Mine is approximately located and possibly gradational
- Jgmr** **Red monzogranite**—Reddish-brown, medium-grained, weakly porphyritic monzogranite forming four small outcrop areas ~1 km east of Foshay Pass. Composed of 35 percent each of red potassium feldspar and greenish-gray plagioclase, 20 percent quartz, and 10 percent mafic minerals and iron oxide. Plagioclase (weakly sericitized) forms small, subhedral phenocrysts ≤5 mm long in a slightly finer grained groundmass (average grain size ~3 mm) of potassium feldspar, quartz, and mafic minerals. Potassium feldspar is poikilitic and contains graphic intergrowths of quartz; mafic minerals are thoroughly altered to chlorite and epidote. One representative sample has ~69 percent SiO₂ and ~9 percent K₂O + Na₂O. Contact with undivided rocks of unit Jg is sharp, but the relative age relations are unclear from field observations
- Jgr** **Altered reddish-brown granitic rocks**—Distinctive zones of altered, deeply weathered, reddish-brown granitic rocks south of Vulcan Mine and west of Goldstone Spring. Rocks are highly fractured, medium-grained (2–4 mm), quartz-rich granitoids characterized by abundant veinlets and irregular masses

of altered biotite and chlorite; some rocks contain no potassium feldspar, presumably because of albitization. Four representative samples contain ~68 to 73 percent SiO₂ and ~5–9 percent K₂O + Na₂O; one of these, which lacks potassium feldspar, is enriched in sodium (~6 percent Na₂O) and depleted in potassium (0.4 percent K₂O) as a result of metasomatism. In many places the altered granitic rocks are cut by small, dark-colored dikes that have not been separately mapped; the alteration of the granitic rocks may be related to intrusion of these dikes. Together, the altered granitic rocks and associated dikes form two narrow, north-trending, recessive outcrop bands surrounded by the more resistant granitoid outcrops of unit Jg; both outcrop bands are offset by east- to northeast-striking, left-lateral strike-slip faults. Smaller, unmapped zones of similarly altered rocks also are present in unit Jg

- Fountain Peak Rhyolite (Jurassic)**—Rhyolite (unit Jfr) associated with sandstone, conglomerate, tuff, and minor limestone (units Jfs, Jfl). Interpreted as part of an intrusive/extrusive rhyolite dome complex (cross section *B–B'*). Unit Jfr samples 12-PR-3713 and 12-PR-3889 yielded late Middle to early Late Jurassic U-Pb zircon ages of 163.6±1.4 Ma and 163.9±1.7 Ma, respectively; Jurassic ages of units Jfs and Jfl are inferred
- Jfr Rhyolite**—Massive, microcrystalline rhyolite that forms resistant outcrops along crest and slopes of Providence Mountains in vicinity of Fountain Peak and Edgar Peak. Dominant rock type is aphanitic to porphyritic rhyolite that varies in color from dark reddish brown and dark reddish purple to light gray, light yellowish gray, and light brownish gray. The rhyolite commonly contains 5–10 percent feldspar phenocrysts (mainly plagioclase) <1 mm to 3 mm long; such phenocrysts rarely form as much as 30 percent of the rock volume. This rhyolite varies from featureless to strongly flow banded, with flow banding ranging from planar to contorted. Less abundant is massive rhyolite that contains scattered to abundant volcanic lithoclasts mostly 1–2 cm but locally as much as 30 cm in maximum dimension; some highly flattened lithoclasts are probably altered pumice fragments. These rocks, which are interpreted to have originated as tuff and welded tuff, are most common in eastern part of outcrop area. Chemically, 15 samples from various parts of unit are all rhyolite having ~70–78 percent SiO₂ and ~9–11 percent total alkalis; only one of these has less than ~74 percent SiO₂.
- Unit is interpreted to contain both intrusive and extrusive components as originally recognized by Hazzard (1954). Rhyolite in western part of outcrop area, including the narrow northern end, cuts across and intrudes adjacent sedimentary units (PIPb, Tms, Tml, Jfs) and is interpreted to represent the feeder system of an extrusive dome represented by rhyolite to the east that is in close spatial association with tuffaceous and sedimentary rocks. Extrusive rocks presumably were once present west of feeder system as well, but later removed by erosion
- Jfs Sandstone, conglomerate, and tuff**—Lenticular sequences of well-bedded clastic rocks below and within rhyolite of unit Jfr. Sequences below unit Jfr overlie Moenkopi Formation or limestone-clast conglomerate (unit JTC) and are overlain or intruded by unit Jfr; sequences within Jfr are in apparent depositional contact with rhyolite above and below, although the mapped contacts are approximately located. Some outcrops are fault bounded.

Dominant rock type is maroon to brown, fine- to coarse-grained, arkosic to volcanic-lithic sandstone composed primarily of detrital feldspar, felsic volcanic grains, and quartz; feldspar grains are commonly subhedral to nearly euhedral, implying little reworking prior to deposition; very fine grained quartz sand and silt are common in the matrix of some coarse-grained sandstones. Many beds display size-sorted, planar lamination. Associated conglomeratic rocks contain granules to small pebbles of volcanic rocks (primarily felsic but also some dark clasts), sandstone, and limestone. South of Crystal Spring on east side of the Providence Mountains, unit is composed primarily of felsic tuff and tuffaceous sandstone, including distinctive green, well-bedded rocks in which diverse, poorly sorted, angular to subangular clasts ranging from fine sand size to 3 mm in diameter are enclosed in a fine-grained felsitic matrix or groundmass; clasts include feldspar, quartz, and fine-grained volcanic and sedimentary lithic fragments. Identical green tuffaceous rocks also form a Quaternary landslide mass downslope of these outcrops. North of Foshay Pass, basal part of unit locally consists of dark-brown, porphyritic andesite that directly overlies Moenkopi Formation; this andesite is overlain by light-gray felsic tuff that is overlain in turn by conglomeratic sandstone. Unit thickness variable, but locally >100 m

- Jfl** **Limestone**—Brownish-gray, massive limestone that forms a narrow, fault-bounded outcrop spatially associated with units **Jfs** and **Jfr** in southeastern part of map area. Origin unknown, possibly an alteration product
- Jfc** **Limestone-clast conglomerate (Jurassic or Triassic)**—Massive to weakly bedded limestone-clast conglomerate, ~10–20 m thick, directly overlying Moenkopi Formation near crest of Providence Mountains northwest of Edgar Peak. Limestone clasts are mostly light-gray, angular to subrounded, and range in size from pebbles to boulders; some contain lenticular chert. Reddish-brown, fine-grained sandstone pebbles and cobbles are subordinate. Clasts are segregated into weakly developed size-sorted layers; elongate clasts generally parallel bedding. Limestone and sandstone clasts probably were derived from the Bird Spring and Moenkopi Formations, respectively
- Moenkopi Formation (Triassic)**—Limestone, sandstone, and minor siltstone and shale. Maximum exposed thickness about 260 m, but absent in many places where Fountain Peak Rhyolite is in direct contact with Bird Spring Formation
- Trml** **Limestone member**—Light- to medium-gray, thin- to medium-bedded limestone and minor interbedded, brown to reddish-brown, fine-grained sandstone, siltstone, and shale. Limestone is characterized by a distinctive nodular texture that produces irregular, wavy bedding surfaces. Fragmented shell material present locally. Present only northwest of Edgar Peak. Thickness ~150 m
- Trms** **Sandstone member**—Predominantly light-brown, thin-bedded, fine-grained calcareous sandstone to siltstone; minor reddish-brown shale and light- to medium-gray, nodular limestone. Sandstone is composed of subequal amounts of detrital quartz and calcite, along with subordinate detrital feldspar, in calcite cement. Lower contact sharp and presumably unconformable. Thickness ~110 m
- PIPb** **Bird Spring Formation (Permian and Pennsylvanian)**—Predominantly limestone, cherty limestone, dolomitic limestone, and dolomite; minor silty limestone and calcareous siltstone. Carbonate rocks are metamorphosed to marble near

plutonic rocks (unit Jg) in southern part of map area. Formation is broadly divisible into upper, middle, and lower parts of approximately equal thickness. Upper part is composed primarily of light-gray, thin- to medium-bedded dolomite and dolomitic limestone that contain irregular, popcorn-shaped, light-gray chert nodules; light- to medium-gray limestone and grayish-orange silty limestone to calcareous siltstone are subordinate. Middle part is composed primarily of light- to medium-gray, thin- to thick-bedded and massive limestone and subordinate grayish-orange silty limestone to calcareous siltstone; marine fossils including fusulinids, solitary corals, and colonial corals are locally abundant (Thompson and Hazzard, 1946; Wilson, 1994; Stevens and Stone, 2007). Lower part is composed of medium- to dark-gray, thick-bedded to massive limestone that commonly contains abundant lenses and nodules of dark-brown chert, including rare spherical to subspherical nodules (“golf ball chert”). Conodonts from middle and lower parts of formation were described by Law (1969). Basal 20 m of formation locally consists of dark-gray, thin-bedded limestone that contains brown, irregularly shaped, phosphatic nodules like those observed at the same stratigraphic position in the Ship Mountains 55 km to the southeast (Stone and others, 2013). Contact with underlying Monte Cristo Limestone is commonly difficult to locate precisely, especially where the dark-gray Yellowpine Member is present; mapped contact was mainly interpreted from aerial photographs based on the geomorphic distinction between the cliff-forming Monte Cristo Limestone and the ledge-and-slope-forming Bird Spring Formation. Total thickness of formation is ~975 m. In addition to bedrock outcrops, unit forms two Quaternary or Pliocene landslide masses, one on each side of the Providence Mountains

Mm Monte Cristo Limestone (Mississippian)—Limestone, cherty limestone, and minor dolomite. From top to bottom, consists of Yellowpine, Bullion, Anchor, and Dawn Members (Hazzard, 1954). Yellowpine Member (maximum thickness about 25 m) consists of medium- to dark-gray limestone locally containing abundant brachiopods, solitary corals, and colonial corals. This unit is absent or unrecognizable at many localities and may be lenticular. Bullion Member, about 100 m thick, consists of light-gray, massive, cliff-forming limestone and minor dolomite containing lenses and nodules of cream-colored chert. Anchor Member, about 70 m thick, consists of light- to dark-gray limestone and minor dolomite containing abundant layers and lenses of brown chert 5–10 cm thick; chert makes up as much as ~40 percent of this unit. Limestone typically becomes lighter in color from bottom to top within the Anchor Member; upper and lower contacts are gradational. Dawn Member, about 70 m thick, consists primarily of medium- to dark-gray limestone that locally contains solitary corals, coarse crinoid debris, and other marine fossil material. Base of member and formation is herein placed at base of a 7-m-thick layer of brownish-gray, sandy dolomite that sharply overlies orthoquartzite mapped as the uppermost part of the Sultan Limestone (unit DI); this sandy dolomite is overlain by 25 m of light-gray, thick-bedded, fine-grained limestone, which in turn is overlain by medium-gray dolomite that grades upward into typical medium- to dark-gray limestone of the Dawn Member. Average total thickness of formation is ~250 m

DI Limestone, dolomite, and quartzite (Devonian)—Informal unit that commonly forms prominent cliffs. Upper half of unit, equivalent to Crystal Pass Member of the Sultan Limestone (Hazzard, 1954), consists primarily of light-gray, light-yellowish-gray, and light-bluish-gray, medium- to thick-bedded, laminated, very fine grained limestone. Late Devonian (Famennian) conodonts were reported in these rocks by Miller (1983). As mapped herein, upper 5 m locally consists of light-gray, medium-grained orthoquartzite that may correlate with the Late Devonian Quartz Spring Member of the Lost Burro Formation of Langenheim and Tischler (1960); in contrast, Hazzard (1954) mapped this orthoquartzite as the basal part of the overlying Monte Cristo Limestone. Lower half of unit, equivalent to upper part of the Valentine Member of the Sultan Formation (Hazzard, 1954), consists primarily of light- to dark-gray, thick-bedded to massive limestone and dolomite, along with minor silty to sandy dolomite and light-gray orthoquartzite. Limestone generally is more abundant than dolomite, although dolomite predominates in some areas. Stromatoporoids are abundant in several limestone and dolomite beds; corals, brachiopods, and gastropods are also present. Late Devonian (Frasnian) conodonts and brachiopods were reported by Miller (1983). Lower 20 m of unit typically consists of massive, light-gray limestone or dolomite overlain by a prominent bed of dark-gray limestone or dolomite 1–2 m thick containing abundant stromatoporoids; these rocks sharply overlie the slope-forming, thinner bedded rocks in the upper part of unit D€d. This prominent lower contact is the most consistent and readily mapped break in the stratigraphic sequence between the Dunderberg Shale and Monte Cristo Limestone. Unit thickness generally ~230 m, but locally as little as ~135 m (see cross section *B-B'*) owing to abrupt lateral thinning of the lower part; map relations suggest that this thinning could have taken place across faults active at the time of deposition

D€d Dolomite, sandy dolomite, and quartzite (Devonian to Cambrian)—Informal unit consisting of an upper and a lower part. Upper 30 to 40 percent of unit consists of thin- to thick-bedded to massive, light- to medium-gray, brown, and grayish-orange dolomite and sandy dolomite, minor light-gray, fine-grained quartzite, and one or two resistant beds of black dolomite 5 to 15 m thick near the middle. The black dolomite beds locally contain poorly preserved stromatoporoids. Lower 60 to 70 percent of unit consists of thick-bedded to massive, light- to dark-gray dolomite that typically weathers to resistant crags and ledges. The dolomite typically forms alternating thick intervals of relatively lighter and darker color; thicknesses of five such intervals that compose one exceptionally well exposed section are, from top to bottom, 30 m (medium gray), 30 m (light gray), 40 m (medium to dark gray), 35 m (light gray), and 70 m (medium gray). Plane-laminated, medium- to coarse-grained dolomite is common in the basal 10 m of unit. Total thickness ~350–390 m.

Lower contact is generally sharp but locally gradational with dolomite in upper part of Dunderberg Shale (€d). Unmapped internal contact between upper and lower parts of unit is indistinct and probably gradational. Black dolomite beds in upper part of unit are equivalent to Ironside Member of the Sultan Limestone and have yielded conodonts of late Middle to early Late

Devonian age (Miller, 1983); these beds are discontinuous and could not be used as a basis for mapping the base of the Sultan Limestone. Rocks above the black dolomite are equivalent to lower part of the Valentine Member of the Devonian Sultan Limestone (Hazzard, 1954; Miller, 1983), and rocks below the black dolomite are interpreted as equivalent to the Devonian and Ordovician Mountain Springs Formation of Miller and Zilinsky (1981). Lower part of unit is equivalent to the Cambrian Cornfield Springs Formation of Palmer and Hazzard, 1956) excluding the basal Dunderberg Shale Member, which here is mapped as a separate formation

- €d **Dunderberg Shale (Cambrian)**—Shale, siltstone, fine-grained sandstone, and dolomite. Upper half to two-thirds of unit consists of light-brown to yellowish-brown, medium- to thick-bedded, coarse-grained dolomite and thin-bedded siltstone and fine-grained sandstone; lower one-third to half of unit consists of dark-greenish-brown to yellowish-brown shale. Forms recessive slopes interrupted by resistant, discontinuous dolomite ledges in upper part of unit. Lower contact sharp. Thickness ~10–30 m
- Bonanza King Formation (Cambrian)**—Dolomite, limestone, and minor silty dolomite; total thickness ~700 m. Forms steep slopes and cliffs above the recessive Cadiz Formation
- €bu **Upper member**—Predominantly light-gray, medium- to thick-bedded, unlaminated to plane-laminated dolomite that sharply overlies the Silver King Dolomite Member. Locally includes thin layers of medium- to dark-gray dolomite and brown siliceous rock. Abundant pisoliths ≤ 0.75 cm in diameter were observed at one locality. Thickness ~80 m
- €bs **Silver King Dolomite Member**—Black to dark-gray dolomite. General appearance massive, but bedding is locally well defined by parting planes, alternating layers of slightly different color 5–20 cm thick, and planar lamination. The dark dolomite commonly contains abundant irregular, narrow fragments or secondary growths of white dolomite as much as 5 cm long, in addition to irregular patches of light-gray dolomite that could be burrow mottling. Peloids or intraclasts were observed locally. A prominent layer of white dolomite 5 to 10 m thick is typically present at or just below top of unit. Basal contact of unit is sharp. Thickness ~100 m
- €bb **Banded Mountain Member**—Dolomite and minor limestone. Primarily light- to dark-gray, thin- to thick-bedded dolomite characterized by well-developed bedding and lamination. Bedding defined by layers of alternating shades of gray, brownish-gray, and yellowish-gray that create a distinctive color-banded appearance or by parting planes in thick sequences of uniform color. Most beds, especially those of relatively light color, are strongly laminated; most lamination is planar, but some is undulatory or domiform which suggests a possible stromatolitic origin. Brown chert lenses are present in many beds, especially those of light-gray color; in addition, some beds contain large, domiform masses of brown chert that could be silicified stromatolites. A few beds contain yellowish-brown silty laminae. Upper 40 to 45 percent of unit is predominantly light to medium gray; lower 55 to 60 percent is predominantly medium to dark gray. Lower part of unit includes a distinctive sequence of medium- to dark-gray limestone several tens of meters thick; this limestone is characterized by irregular laminae and thin beds of light-gray dolomite that

create a mottled appearance, similar to limestone of the underlying Papoose Lake Member. Lowermost 5 to 10 m of member typically consists of very dark gray, massive, ledge-forming dolomite that sharply overlies the recessive beds at top of the Papoose Lake Member. Thickness ~300 m

- €bp **Papoose Lake Member**—Limestone, dolomite, and silty dolomite. Upper half of unit is composed primarily of light- to medium-gray, thin- to thick-bedded, laminated dolomite and minor brown-weathering silty dolomite. Uppermost 20 m is a distinctive zone of orange-weathering, thin-bedded and laminated, silty dolomite that forms recessive slopes between the more resistant rocks above and below. Lower half of unit is composed of medium- to dark-gray, thin-bedded limestone that grades upward into buff and medium- to dark-gray, thin- to thick-bedded dolomite. Limestone beds are 1–5 cm thick and separated by irregular partings and interbeds of light-gray, brown, and yellowish-brown dolomite that create a distinctive color-banded appearance and mottled bedding surfaces. Some limestone contains small bioclastic fragments. Lower contact gradational with calcareous upper part of the Cadiz Formation. Thickness ~220 m
- €c **Cadiz Formation (Cambrian)**—Lithologically heterogeneous unit composed of shale, siltstone, sandstone, and limestone. Uppermost ~30 m of unit consists of moderately resistant, thin-bedded, medium- to dark-gray or bluish-gray limestone and yellowish-brown mudstone that form alternating layers 1–4 cm thick with irregular margins. Underlying rocks are primarily maroon, yellow, yellowish-brown, and olive-green shale and yellowish-brown to dark-brown, thin-bedded and laminated siltstone to fine-grained sandstone and calcareous sandstone that form recessive slopes. Scattered, more resistant beds of light-gray to brownish-gray, plane- to cross-laminated, sandy and (or) oolitic limestone as much as 1 m thick form ribs across these slopes. Lower contact of formation is sharp. Thickness ~145 m
- €cs **Siltstone unit**—Distinctive unit of dark-purple, ripple-marked siltstone ~10 m thick present locally near middle of formation
- €ch **Chambless Limestone (Cambrian)**—Medium- to dark-gray, thin-bedded to massive limestone characterized by abundant spherical to subspherical algal nodules (oncolites) 2 to 3 cm in diameter (“*Girvanella*” sp. of Hazzard, 1954). Forms resistant ledges within which bedding is defined by parting planes or by irregular laminae of yellowish-brown mudstone or siltstone. Lower contact sharp. Thickness ~65 m
- €l **Latham Shale (Cambrian)**—Brown to greenish-brown, fissile shale and siltstone; subordinate thin-bedded sandstone. Forms recessive slopes; lower contact sharp. Thickness ~10–20 m
- €z **Zabriskie Quartzite (Cambrian)**—Light-gray, massive, medium-grained orthoquartzite that typically forms resistant, reddish-brown-weathering outcrops. Locally plane laminated. Lower contact sharp. Regarded as upper part of the Prospect Mountain Quartzite by Hazzard (1954); identified as Zabriskie Quartzite by Stewart (1970). Thickness ~25–35 m
- €Zu **Wood Canyon Formation and Stirling Quartzite, undivided (Cambrian and Neoproterozoic)**—Quartzite and subordinate siltstone. Upper half of unit, corresponding approximately to the Wood Canyon Formation, is composed of

reddish-brown-weathering, fine- to medium-grained, thin- to thick-bedded quartzite and minor interbedded siltstone. The quartzite is characterized by ubiquitous planar and cross lamination; detrital grains are well sorted, tightly packed, and include minor feldspar and mica in addition to the dominant quartz. Lower half of unit, corresponding approximately to the Stirling Quartzite, is primarily composed of thick-bedded to massive, light-gray to cream-colored, medium- to coarse-grained quartzite and conglomeratic quartzite that locally contain angular to rounded quartzite clasts as much as 3 cm in diameter. The moderately sorted to well-sorted quartzite contains 2–5 percent detrital feldspar that is mostly microcline but also includes minor plagioclase; some quartzite has a calcareous cement. This thick-bedded to massive quartzite typically forms an upper and a lower sequence of resistant strata separated by a middle, less resistant sequence of medium- to dark-gray, thin-bedded, fine-grained quartzite and siltstone. Lower contact of unit is sharp. Unit was regarded as the middle part of the Prospect Mountain Quartzite by Hazzard; identified as Wood Canyon Formation and Stirling Quartzite by Stewart (1970), who also noted the inconspicuous and subtle contact between these two formations in this area. No attempt to define and map an interformational contact was made during the present study. Total unit thickness is ~300 m

- Zj **Johnnie Formation (Neoproterozoic)**—Dolomite, limestone, and quartzite. Upper 15 to 20 m consists of light-gray, grayish-orange, brownish-gray, and reddish-gray, medium- to thick-bedded, laminated, sandy carbonate rocks that vary laterally from limestone to dolomite. Lower 5 to 10 m consists of light-gray, massive, medium-grained orthoquartzite that contains 1–2 percent detrital feldspar and rare muscovite and heavy minerals. Basal orthoquartzite rests unconformably on underlying metamorphic rocks (unit Xm); contact commonly disturbed by minor, unmapped faults. Unit forms recessive slopes below overlying, resistant quartzite (lower part of unit €Zu); in one small area near Cornfield Spring, unit is absent apparently as a result of faulting and erosion prior to deposition of unit €Zu. Regarded as lower part of Prospect Mountain Quartzite by Hazzard (1954); identified as Johnnie Formation by Stewart (1970). Thickness ~20–30 m
- Xq **Quartz veins or dikes (Paleoproterozoic?)**—Elongate, tabular bodies of white to purple quartz as much as 10 m thick that cut rocks of unit Xm in northern part of map area
- Xm **Metamorphic and plutonic rocks, undivided (Paleoproterozoic)**—Gneiss, granitoid rocks, pegmatite, and quartz-rich metasedimentary(?) or metavolcanic(?) rocks; unit forms featureless slopes in contrast to overlying well-bedded sedimentary rocks. Dominant rock type is strongly foliated, fine-grained, equigranular, quartz-feldspar-biotite gneiss composed of alternating felsic and mafic layers 1–4 mm thick. Thicker layers of predominantly felsic and mafic composition, however, are also common. Felsic layers typically contain subequal amounts of potassium feldspar, plagioclase, and quartz, although potassium feldspar commonly is subordinate or even absent; mafic layers contain as much as 80 percent biotite. Average grain size in most samples is less than 1 mm. Gneissic layers are almost invariably planar; in a few places they are deformed by small-scale folds. Gneiss is undated in map

area but extends northward where it is dated as Paleoproterozoic (~1,710 Ma; Wooden and Miller, 1990; Miller and others, 2007). Gneiss is locally associated with subordinate unfoliated to weakly foliated granitoid rocks and pegmatite. In northwestern part of area and locally along east flank of Providence Mountains near C&K Mine, sizeable parts of unit consist of light-gray to light-brown, unfoliated, fine-grained, equigranular rocks composed of subequal quartz and feldspar (plagioclase \geq potassium feldspar) with few or no mafic minerals; average grain size is less than 1 mm, many quartz grains are rounded, and the texture suggests a sedimentary or possibly volcanic origin. One small outcrop of coarse-grained orthoquartzite was observed near C&K Mine

References Cited

- Barnes, H., Christiansen, R.L., and Byers, F.M., Jr., 1962, Cambrian Carrara Formation, Bonanza King Formation, and Dunderberg Shale east of Yucca Flat, Nye County, Nevada: U.S. Geological Survey Professional Paper 450–D, p. D27–D31.
- Bedford, D.R., Miller, D.M., and Phelps, G.A., 2010, Surficial geologic map of the Amboy 30' x 60' quadrangle, San Bernardino County, California: U.S. Geological Survey Scientific Investigations Map 3109, scale 1:100,000, 26 p.
- Bergmann, K.D., Zentmeyer, R.A., and Fischer, W.W., 2011, The stratigraphic expression of a large negative carbon isotope excursion from the Ediacaran Johnnie Formation, Death Valley: *Precambrian Research*, v. 199, p. 45–56.
- Best, M.G., and Christiansen, E.H., 2001, *Igneous petrology: Malden, Mass.*, Blackwell Science, 458 p.
- Billingsley, G.H., Wenrich, K.J., Huntoon, P.W., and Young, R.A., 1999, Breccia-pipe and geologic map of the southwestern part of the Hualapai Indian Reservation and vicinity, Arizona: U.S. Geological Survey Miscellaneous Investigations Series, Map I–2554, scale 1:48,000, 50 p.
- Buesch, D.C., 1991, Changes in depositional environments resulting from emplacement of a large-volume ignimbrite, *in* Fisher, R.V., and Smith, G.A., eds., *Sedimentation in volcanic settings: Society for Sedimentary Geology (SEPM) Special Publication*, v. 45, p. 139–153.
- Buesch, D.C., 1993, Feldspar geochemistry of four Miocene ignimbrites in southeastern California and western Arizona, *in* Sherrod, D.R., and Nielson, J.E., eds., *Tertiary stratigraphy of highly extended terranes, California, Arizona, and Nevada: U.S. Geological Survey Bulletin 2053*, p. 55–85.
- Bull, W.B., 1991, *Geomorphic responses to climatic change: New York*, Oxford University Press, 326 p.
- Burchfiel, B.C., and Davis, G.A., 1975, Nature and controls of Cordilleran orogenesis, western United States—Extensions of an earlier synthesis: *American Journal of Science*, v. 275–A, p. 363–396.
- Burchfiel, B.C., and Davis, G.A., 1977, Geology of the Sagamore Canyon-Slaughterhouse Spring area, New York Mountains, California: *Geological Society of America Bulletin*, v. 88, p. 1623–1640.
- Burchfiel, B.C., and Davis, G.A., 1981, Mojave Desert and environs, chap. 9 *of* Ernst, W.G., ed., *The geotectonic development of California (Rubey Volume 1): Englewood Cliffs, N.J., Prentice-Hall*, p. 217–252.
- Busby-Spera, C., 1988, Speculative tectonic model for the early Mesozoic arc of the southwest Cordilleran United States: *Geology*, v. 16, p. 1121–1125.
- Dickinson, W.R., 1981, Plate tectonics and the continental margin of California, chap. 1 *of* Ernst, W.G., ed., *The geotectonic development of California (Rubey Volume 1): Englewood Cliffs, N.J., Prentice-Hall*, p. 1–28.
- Dunne, G.C., 1977, Geology and structural evolution of Old Dad Mountain, Mojave Desert, California: *Geological Society of America Bulletin*, v. 88, p. 737–748.
- Ferguson, C.A., McIntosh, W.C., and Miller, C.F., 2013, Silver Creek caldera—The tectonically dismembered source of the Peach Spring Tuff: *Geology*, v. 41, no. 1, p. 3–6.
- Fox, L.K., and Miller, D.M., 1990, Jurassic granitoids and related rocks of the southern Bristol Mountains, southern Providence Mountains, and Colton Hills, Mojave Desert, California, *in* Anderson, J.L., ed., *The nature and origin of Cordilleran magmatism: Geological Society of America Memoir 174*, p. 111–132.
- Gans, W.T., 1974, Correlation and redefinition of the Goodsprings Dolomite, southern Nevada and eastern California: *Geological Society of America Bulletin*, v. 85, p. 189–200.
- Goldfarb, R.J., Miller, D.M., Simpson, R.W., Hoover, D.B., Moyle, P.R., Olson, J.E., and Gaps, R.S., 1988, Mineral resources of the Providence Mountains Wilderness Study Area, San Bernardino County, California: U.S. Geological Survey Bulletin 1712–D, p. D1–D70.

- Gusa, S., Nielson, J.E., and Howard, K.A., 1987, Heavy-mineral suites confirm the wide extent of Peach Springs Tuff in California and Arizona, U.S.A.: *Journal of Volcanology and Geothermal Research*, v. 33, p. 343–347.
- Hamilton, W., 1969, Mesozoic California and the underflow of Pacific mantle: *Geological Society of America Bulletin*, v. 80, p. 2409–2430.
- Haxel, G.B., and Miller, D.M., 2007, Mesozoic rocks, *in* Theodore, T.G., ed., *Geology and mineral resources of the East Mojave National Scenic Area, San Bernardino County, California*: U.S. Geological Survey Bulletin 2160, p. 59–66.
- Hazzard, J.C., 1954, Rocks and structure of the northern Providence Mountains, San Bernardino County, California, *in* Jahns, R.H., ed., *Geology of southern California: California Division of Mines Bulletin* 170, ch. 4, no. 4, p. 27–35, and pl. 2 (geologic map, scale ~1:31,572).
- Hazzard, J.C., and Crickmay, C.H., 1933, Notes on the Cambrian rocks of the eastern Mohave Desert, California: *University of California Publications, Department of Geological Sciences Bulletin*, v. 23, no. 2., p. 57–80.
- Hazzard, J.C., and Mason, J.F., 1936, Middle Cambrian formations of the Providence and Marble Mountains, California: *Geological Society of America Bulletin*, v. 47, p. 228–240.
- Hewett, D.F., 1956, *Geology and mineral resources of the Ivanpah quadrangle, California and Nevada*: U.S. Geological Survey Professional Paper 275, 172 p., scale 1:125,000.
- Langenheim, R.L., Jr., and Tischler, H., 1960, Mississippian and Devonian paleontology and stratigraphy, Quartz Spring area, Inyo County, California: *University of California Publications in Geological Sciences*, v. 38, no. 2, p. 89–150.
- Langenheim, V.E., Biehler, S., Negrini, R., Mickus, K., Miller, D.M., and Miller, R.J., 2009, Gravity and magnetic investigations of the Mojave National Preserve and adjacent areas, California and Nevada: U.S. Geological Survey Open-File Report 2009–1117, 25 p.
- Law, B.E., 1969, Pennsylvanian–Permian conodont succession from the Bird Spring Formation, southeastern California: San Diego, Calif., San Diego State College, M.S. thesis, 84 p.
- LeMaitre, R.W., Streckeisen, A., Zanettin, B., and 12 others, eds., 2002, *Igneous rocks, a classification and glossary of terms*: Cambridge, U.K., Press Syndicate of the University of Cambridge, 236 p.
- Loyd, R.C., 1993, Mineral land classification of the Kerens, Flynn, and Colton Well 15-minute quadrangles, San Bernardino County, California: *California Division of Mines and Geology Special Report* 168, 85 p.
- Ludwig, K., 2008, User’s manual for Isoplot 3.70, a geochronological toolkit for Microsoft Excel: Berkeley Geochronology Center Special Publication 4, 76 p.
- Ludwig, K., 2009, Squid 2, Rev. 2.50, a user’s manual: Berkeley Geochronology Center Special Publication 5, 110 p.
- McCurry, M., 1985, The petrology of the Woods Mountains Volcanic Center, San Bernardino County, California: Los Angeles, University of California, Ph.D. dissertation, 403 p.
- McCurry, M., 1988, Geology and petrology of the Woods Mountains Volcanic Center, southeastern California—Implications for the genesis of peralkaline rhyolite ash flow tuffs: *Journal of Geophysical Research*, v. 93, no. B12, p. 14,835–14,855.
- McCurry, M., Lux, D.R., and Mickus, K.L., 1995, Neogene structural evolution of the Woods Mountains Volcanic Center, East Mojave National Scenic Area, *in* Reynolds, R.E., and Reynolds, J., eds., *Ancient surfaces of the east Mojave Desert*: San Bernardino County Museum Association Quarterly, v. 42, no. 3, p. 75–80.
- McDonald, E., and McFadden, L.D., 1994, Quaternary stratigraphy of the Providence Mountains piedmont and preliminary age estimates and regional stratigraphic correlations of Quaternary deposits in the eastern Mojave Desert, California, *in* Wells, S.C., Tinsley, J.C., McFadden, L.D., and Lancaster, N., *Quaternary stratigraphy and dating methods—Understanding geologic processes and landscape*

- evolution in southern California, Trip 8 of McGill, S.F., and Ross, T.M., eds., Geological investigations of an active margin: Geological Society of America Cordilleran Section Guidebook, 27th Annual Meeting, San Bernardino, Calif., p. 205–210.
- McDonald, E.V., McFadden, L.D., and Wells, S.G., 1995, The relative influence of climate change, desert dust, and lithologic control on soil-geomorphic processes on alluvial fans, Mojave Desert, California—Summary of results, *in* Reynolds, R.E., and Reynolds, J., eds., Ancient surfaces of the east Mojave Desert: San Bernardino County Museum Association Quarterly, v. 42, no. 3, p. 35–42.
- Miller, D.M., 2012, Surficial geologic map of the Ivanpah 30' x 60' quadrangle, San Bernardino County, California, and Clark County, Nevada: U.S. Geological Survey Scientific Investigations Map 3206, scale 1:100,000, 14 p.
- Miller, D.M., Glick, L.L., Goldfarb, R., Simpson, R.W., Hoover, D.B., Detra, D.E., Dohrenwend, J.C., and Munts, S.R., 1985, Mineral resources and resource potential map of the South Providence Mountains Wilderness Study Area, San Bernardino County, California: U.S. Geological Survey Miscellaneous Field Studies Map MF-1780A, scale 1:62,500, 29 p.
- Miller, D.M., Miller, R.J., Nielsen, J.E., Wilshire, H.G., Howard, K.A., and Stone, Paul, 1991, Preliminary geologic map of the East Mojave National Scenic Area, California: U.S. Geological Survey Open-File Report 91-435, scale 1:100,000.
- Miller, D.M., Miller, R.J., Nielsen, J.E., Wilshire, H.G., Howard, K.A., and Stone, Paul, 2007, Geologic map of the East Mojave National Scenic Area, California, *in* Theodore, T.G., ed., Geology and mineral resources of the East Mojave National Scenic Area, San Bernardino County, California: U.S. Geological Survey Bulletin 2160, scale 1:125,000.
- Miller, D.M., Wells, M.L., Dewitt, E., Walker, J.D., and Nakata, J.K., 1996, Late Cretaceous extensional fault system across the northeastern Mojave Desert, *in* Reynolds, R.E., and Reynolds, J., eds., Punctuated chaos in the northeastern Mojave Desert: San Bernardino County Museum Association Quarterly, v. 43, no. 1, p. 77–84.
- Miller, J.M., 1983, Devonian stratigraphy of the northern Providence Mountains, San Bernardino County, California: Riverside, University of California, M.S. thesis, 121 p.
- Miller, R.H., and Zilinsky, G.A., 1981, Lower Ordovician through Lower Devonian cratonic margin rocks of the southern Great Basin: Geological Society of America Bulletin, part 1, v. 92, p. 255–261.
- Palmer, A.R., and Hazzard, J.C., 1956, Age and correlation of Cornfield Springs and Bonanza King Formations in southeastern California and southern Nevada: American Association of Petroleum Geologists Bulletin, v. 40, no. 10, p. 2494–2513.
- Sarna-Wojcicki, A.M., Reheis, M.C., Pringle, M.S., Fleck, R.J., Burbank, D., Meyer, C.E., Slate, J.L., Wan, E., Budahn, J.R., Troxel, B., and Walker, J.P., 2005, Tephra layers of Blind Spring Valley and related upper Pliocene and Pleistocene tephra layers, California, Nevada, and Utah—Isotopic ages, correlation, and magnetostratigraphy: U.S. Geological Survey Professional Paper 1701, 63 p.
- Sherrod, D.R., and Nielson, J.E., eds., 1993, Tertiary stratigraphy of highly extended terranes, California, Arizona, and Nevada: U.S. Geological Survey Bulletin 2053, 250 p.
- Stevens, C.H., and Stone, Paul, 2007, The Pennsylvanian–Early Permian Bird Spring carbonate shelf, southeastern California—Fusulinid biostratigraphy, paleogeographic evolution, and tectonic implications: Geological Society of America Special Paper 429, 82 p.
- Stewart, J.H., 1970, Upper Precambrian and Lower Cambrian strata in the southern Great Basin, California and Nevada: U.S. Geological Survey Professional Paper 620, 206 p.
- Stone, Paul, Stevens, C.H., Howard, K.A., and Hoisch, T.D., 2013, Stratigraphy and paleogeographic significance of the Pennsylvanian–Permian Bird Spring Formation in the Ship Mountains, southeastern California: U.S. Geological Survey Scientific Investigations Report 2013–5109, 40 p.
- Theodore, T.G., ed., 2007, Geology and mineral resources of the East Mojave National Scenic Area, San Bernardino County, California: U.S. Geological Survey Bulletin 2160, 265 p.

- Thompson, M.L., and Hazzard, J.C., 1946, Permian fusulinids of southern California, part 3 of Thompson, M.L., Wheeler, H.E., and Hazzard, J.C., Permian fusulinids of California: Geological Society of America Memoir 17, p. 37–53.
- Wells, M.L., Beyene, M.A., Spell, T.L., Kula, J.L., Miller, D.M., and Zanetti, K.A., 2005, The Pinto shear zone; a Laramide synconvergent extensional shear zone in the Mojave Desert region of the southwestern United States: *Journal of Structural Geology*, v. 27, p. 1697–1720.
- Wells, R.E., and Hillhouse, J.W., 1989, Paleomagnetism and tectonic rotation of the lower Miocene Peach Springs Tuff—Colorado Plateau, Arizona, to Barstow, California: *Geological Society of America Bulletin*, v. 101, no. 6, p. 846–863.
- Wilson, E.C., 1994, Early Permian corals from the Providence Mountains, San Bernardino County, California: *Journal of Paleontology*, v. 68, no. 5, p. 938–951.
- Wooden, J.L., and Miller, D.M., 1990, Chronologic and isotopic framework for Early Proterozoic crustal evolution in the eastern Mojave Desert region, southeastern California: *Journal of Geophysical Research*, v. 95, no. B12, p. 20,133–20,146.
- Young, R.A., and Brennan, W.J., 1974, Peach Springs Tuff—Its bearing on structural evolution of the Colorado Plateau and development of Cenozoic drainage in Mohave County, Arizona: *Geological Society of America Bulletin*, v. 85, no. 1, p. 83–90.

Appendix 1—Sample Localities and Descriptions

Samples from 466 localities in and near the map area are listed and described in table 2. Sample descriptions are based on field observations and qualitative examination of petrographic thin sections and sawn slabs, including many that were stained for potassium feldspar and plagioclase. The majority of samples are from Paleoproterozoic metamorphic rocks, Jurassic plutonic and volcanic rocks, and Miocene volcanic rocks; relatively few are from the Neoproterozoic to Triassic sedimentary rocks, the nature of which could be adequately determined by field observation in most cases. From 2004 to 2014, sample localities were recorded in the field with a hand-held GPS; samples collected in 1985 were located on printed topographic maps from which the latitude and longitude coordinates could be determined.

Table 2. Localities and descriptions of samples from the Providence Mountains in parts of the Fountain Peak and adjacent 7.5' quadrangles, San Bernardino County, California. [Title of table is included here for continuity; complete table is available at <https://doi.org/10.3133/sim3376>.]

Appendix 2—Fossil Identifications

Fossils are present in several of the Cambrian to Triassic sedimentary rock units in the map area. Many significant fossil assemblages were discovered and identified by J.C. Hazzard and colleagues during their pioneering studies of the Providence Mountains (Hazzard and Crickmay, 1933; Hazzard and Mason, 1936; Thompson and Hazzard, 1946; Hazzard, 1954; Palmer and Hazzard, 1956). These fossil identifications provided a solid biostratigraphic framework that has remained essentially unchanged to the present day. A few later studies provided additional paleontological information for some units (Law, 1969; Miller, 1983; Wilson, 1994).

The only fossils studied in any detail during the present investigation are fusulinids from the Pennsylvanian to Early Permian Bird Spring Formation. Fusulinids were collected in 1985, 2004, and 2007–2010. The collections from 1985 and 2004 were included in a regional study of Late Pennsylvanian and early Permian (Cisuralian) fusulinids by Stevens and Stone (2007); those from 2007–2010 are reported here (table 3; fig. 11). All of the samples reported here represent the early Permian (late Asselian to middle Sakmarian) Fusulinid Zone 3 of Stevens and Stone (2007).

Table 3. Fusulinids from the Bird Spring Formation in the Providence Mountains in parts of the Fountain Peak and adjacent 7.5' quadrangles, San Bernardino County, California.

[Fusulinids identified by C.H. Stevens from samples collected by P. Stone from 2007 to 2010. See appendix 1 for sample localities and descriptions]

Locality Number	Sample Number	Fusulinids
07-PR-531	S-2035	<i>Schwagerina modica</i>
07-PR-537	S-2036	<i>Schwagerina aculeata</i>
07-PR-571	S-2048	<i>Schwagerina providens</i> , <i>S. aculeata</i> , <i>Pseudoschwagerina roeseleri</i>
07-PR-1067	S-2091	<i>Schwagerina aculeata</i> , <i>S. wellsensis</i> , <i>Pseudoschwagerina uddeni</i> , <i>P. roeseleri?</i>
09-PR-2611	S-2110	<i>Schwagerina aculeata</i> , <i>S. providens</i> , <i>Pseudoschwagerina roeseleri</i> , <i>Cuniculinella?</i> sp.
10-PR-2818	S-2113	<i>Pseudoschwagerina roeseleri</i> , <i>Stewartina</i> sp.
10-PR-2819	S-2112	<i>Leptotriticites</i> cf. <i>L. californicus</i> , <i>L.</i> cf. <i>L. panamintensis</i> , <i>L.</i> sp., <i>Schwagerina</i> aff. <i>S. modica</i>
10-PR-2876	S-2115	<i>Schwagerina aculeata</i> , <i>S. providens</i> , <i>S. modica</i> , <i>Pseudoschwagerina</i> sp.
10-PR-2877	S-2114	<i>Schwagerina aculeata</i> , <i>S. providens</i> , <i>S. modica</i> , <i>S.</i> sp. 4 of Stevens and Stone (2007), <i>Pseudoschwagerina</i> cf. <i>P. roeseleri</i> , <i>Stewartina</i> sp.
10-PR-3021	S-2116	<i>Schwagerina aculeata</i>
10-PR-3021A	S-2117	<i>Schwagerina</i> cf. <i>S. colemani</i>

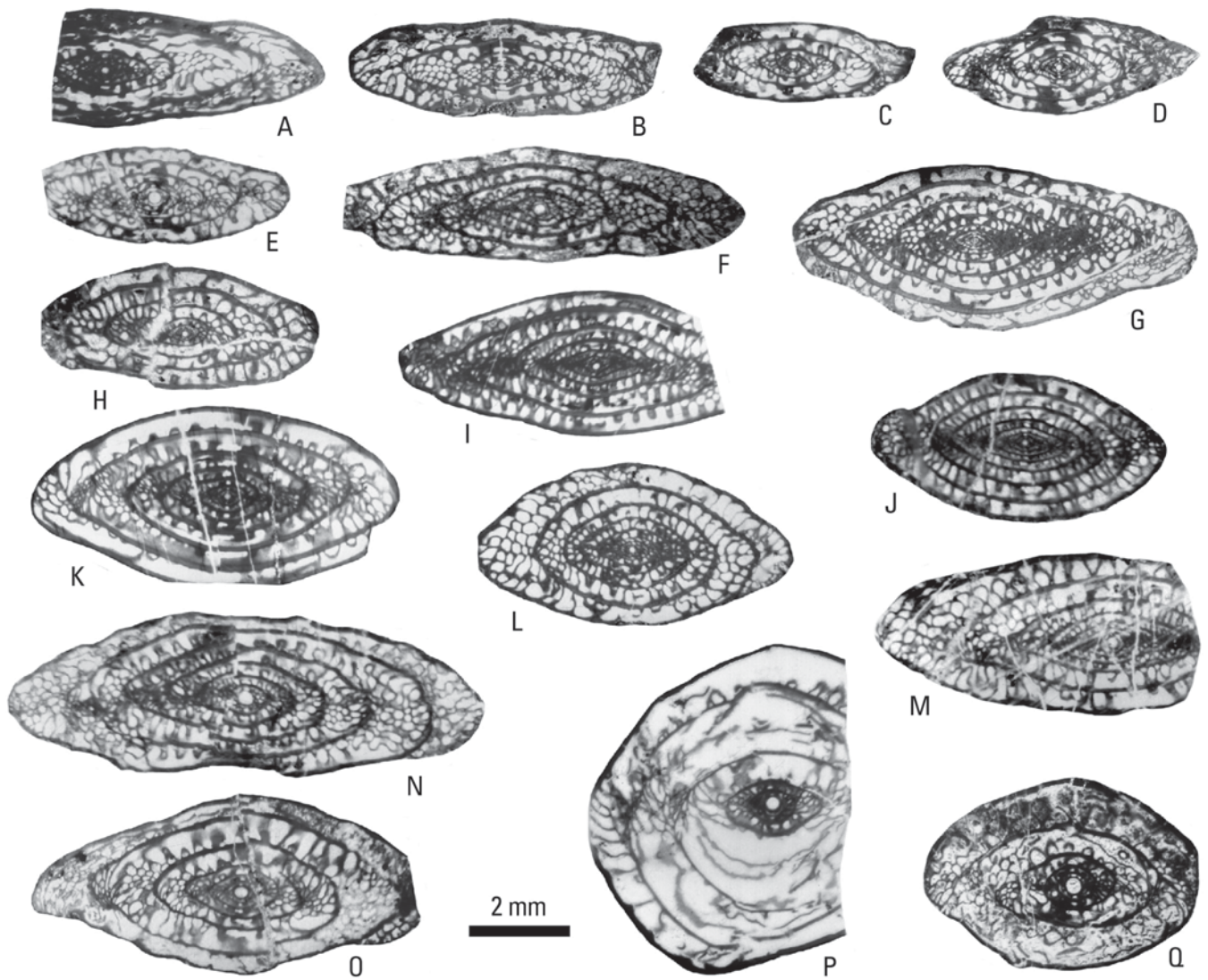


Figure 11. Thin-section photographs of fusulinids from the Bird Spring Formation. All figures are axial sections. Specimens are housed in San Jose State University Museum of Paleontology, San Jose, California. A, *Leptotriticites* sp., sample S-2112. B, C, *Leptotriticites* cf. *L. californicus*, sample S-2112. D, *Leptotriticites* cf. *L. panamintensis*, sample S-2112. E, F, *Schwagerina providens*, sample S-2048. G, *Schwagerina aculeata*, sample S-2116. H, *Schwagerina aculeata?*, sample S-2115. I, *Schwagerina aculeata*, sample S-2110. J, *Schwagerina aculeata*, sample S-2036. K, *Schwagerina aculeata*, sample S-2110. L, *Schwagerina aculeata*, sample S-2116. M, *Schwagerina* sp. 4 of Stevens and Stone (2007), sample S-2114. N, *Schwagerina wellsensis*, sample S-2091. O, *Stewartina* sp., sample S-2113. P, *Pseudoschwagerina roeseleri*, sample S-2110. Q, *Pseudoschwagerina roeseleri*, sample S-2091.

Appendix 3—Geochemical Data

Whole-rock geochemical analyses were obtained for 131 samples of Jurassic and Miocene igneous rocks. The analyses, which were performed under contract to the U.S. Geological Survey, included both wave-length-dispersive X-ray fluorescence (WDXRF) (table 4) and inductively coupled plasma atomic emission spectroscopy (ICP-AES) (table 5). Harker (variation) diagrams plotting oxides of selected elements against silica (SiO₂) are shown in figures 12–15. The geochemical data aided in classifying the igneous rocks, especially those of fine grain size. Pertinent geochemical characteristics are included in the Description of Map Units.

Table 4. X-ray fluorescence geochemical analyses of selected Jurassic and Miocene igneous rock samples from the Providence Mountains in parts of the Fountain Peak and adjacent 7.5' quadrangles, San Bernardino County, California. [Title of table is included here for continuity; complete table is available at <https://doi.org/10.3133/sim3376>.]

Table 5. ICP-AES (inductively coupled plasma atomic emission spectrometry) geochemical analyses of selected Jurassic and Miocene igneous rock samples from the Providence Mountains in parts of the Fountain Peak and adjacent 7.5' quadrangles, San Bernardino County, California. [Title of table is included here for continuity; complete table is available at <https://doi.org/10.3133/sim3376>.]

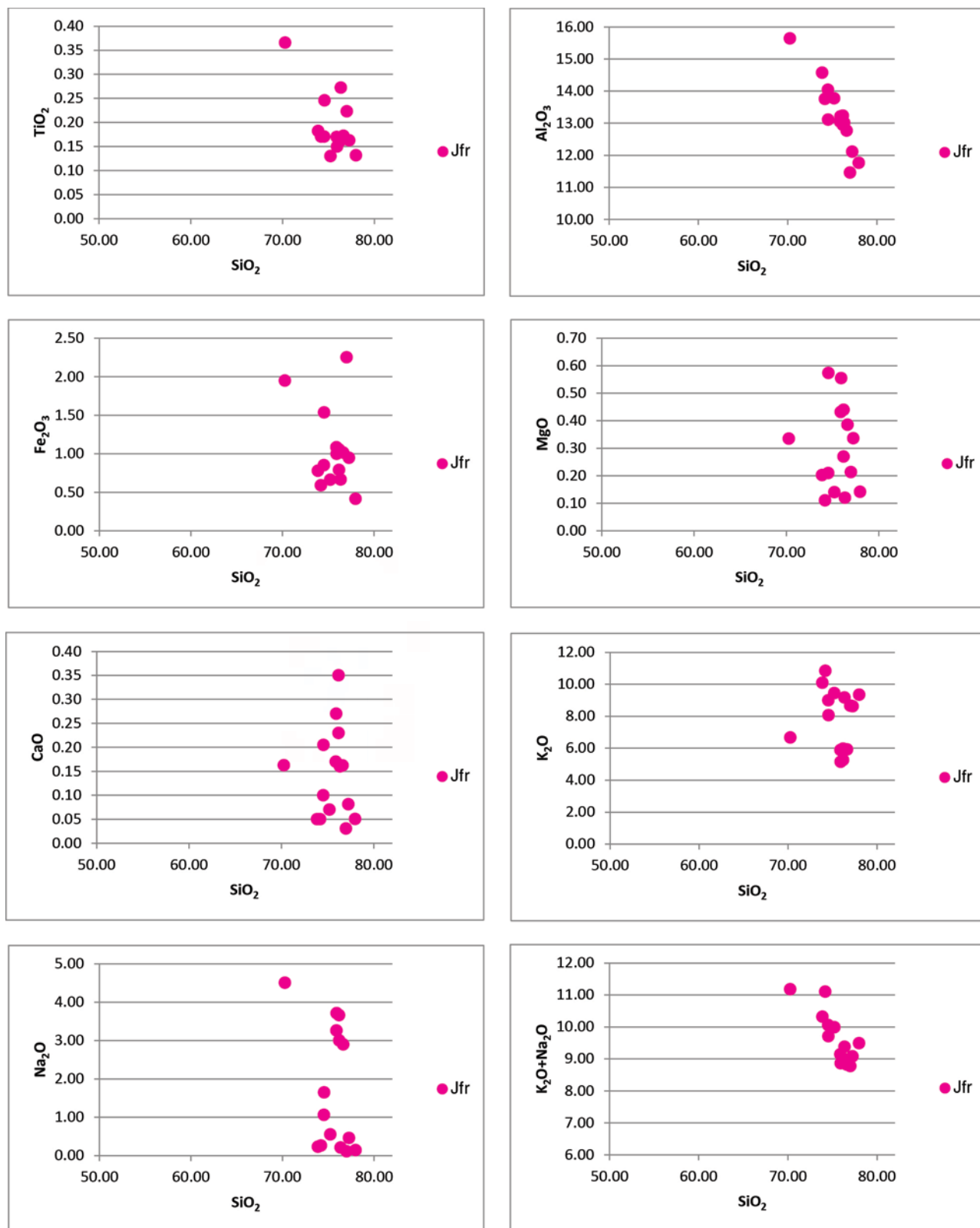


Figure 12. Harker diagrams showing variations in the abundances of selected oxides with respect to silica (SiO₂) in samples from Jurassic map unit Jfr (Fountain Peak Rhyolite). Oxides are titanium (TiO₂), aluminum (Al₂O₃), iron (Fe₂O₃), magnesium (MgO), calcium (CaO), potassium (K₂O), sodium (Na₂O), and potassium + sodium (K₂O+Na₂O). Values are in normalized weight percent.

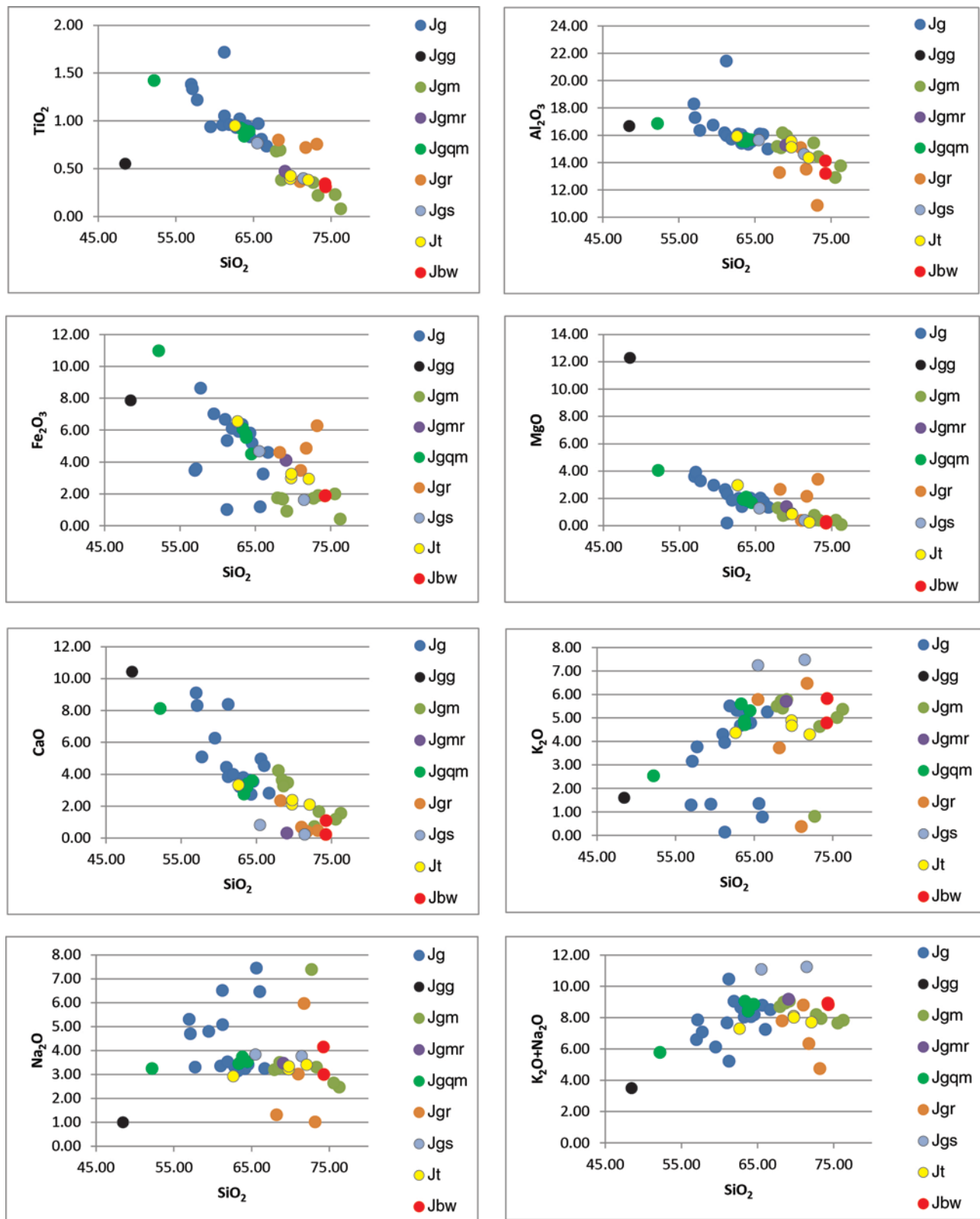


Figure 13. Harker diagrams showing variations in the abundances of selected oxides with respect to silica (SiO₂) in samples from Jurassic plutonic map units Jg, Jgg, Jgm, Jgmr, Jgqm, Jgr, Jgs, Jt, and Jbw (see Description of Map Units for unit names). Oxides are titanium (TiO₂), aluminum (Al₂O₃), iron (Fe₂O₃), magnesium (MgO), calcium (CaO), potassium (K₂O), sodium (Na₂O), and potassium + sodium (K₂O+Na₂O). Values are in normalized weight percent.

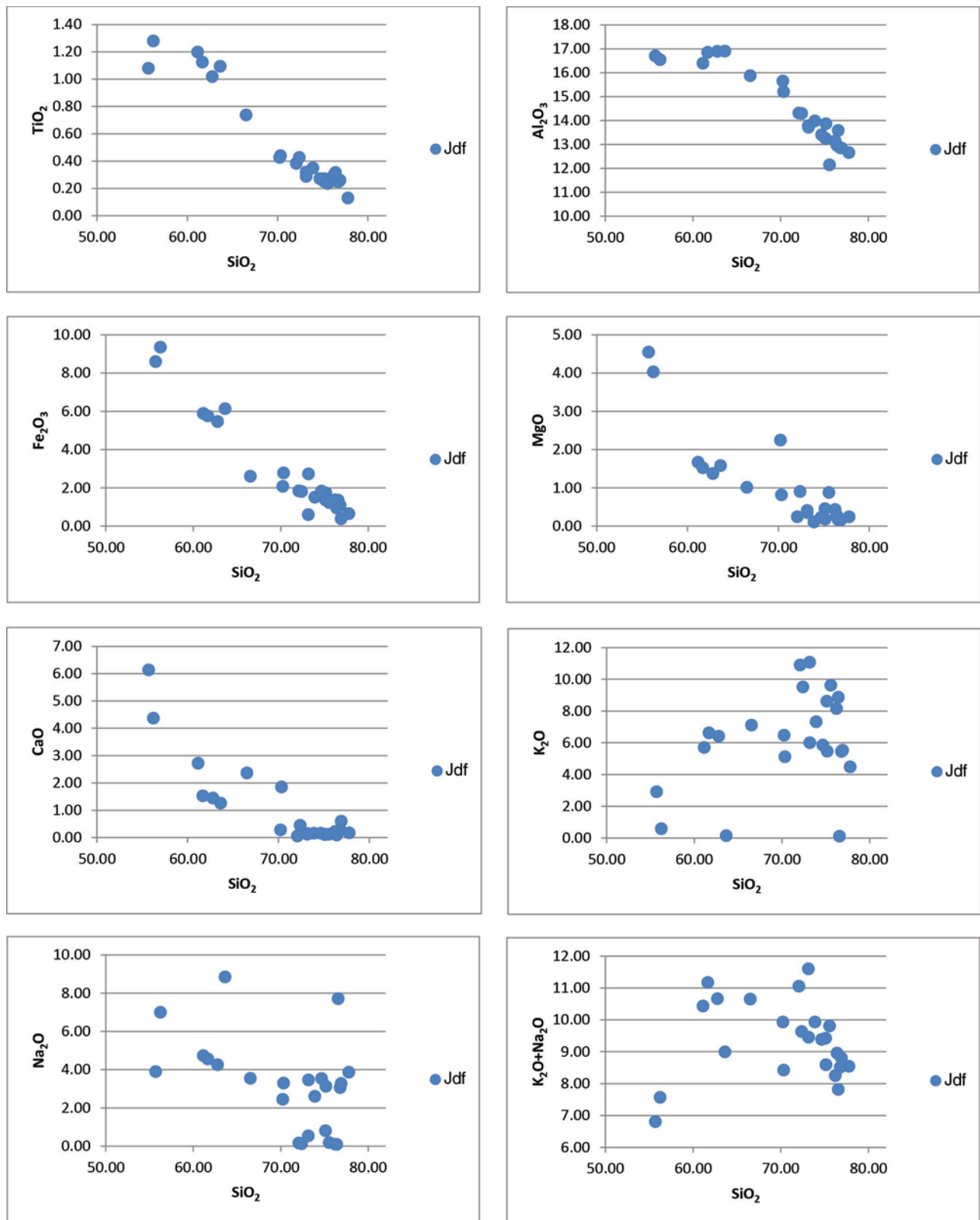


Figure 14. Harker diagrams showing variations in the abundances of selected oxides with respect to silica (SiO₂) in samples from Jurassic map unit Jdf (felsic to intermediate dikes). Oxides are titanium (TiO₂), aluminum (Al₂O₃), iron (Fe₂O₃), magnesium (MgO), calcium (CaO), potassium (K₂O), sodium (Na₂O), and potassium + sodium (K₂O+Na₂O). Values are in normalized weight percent.

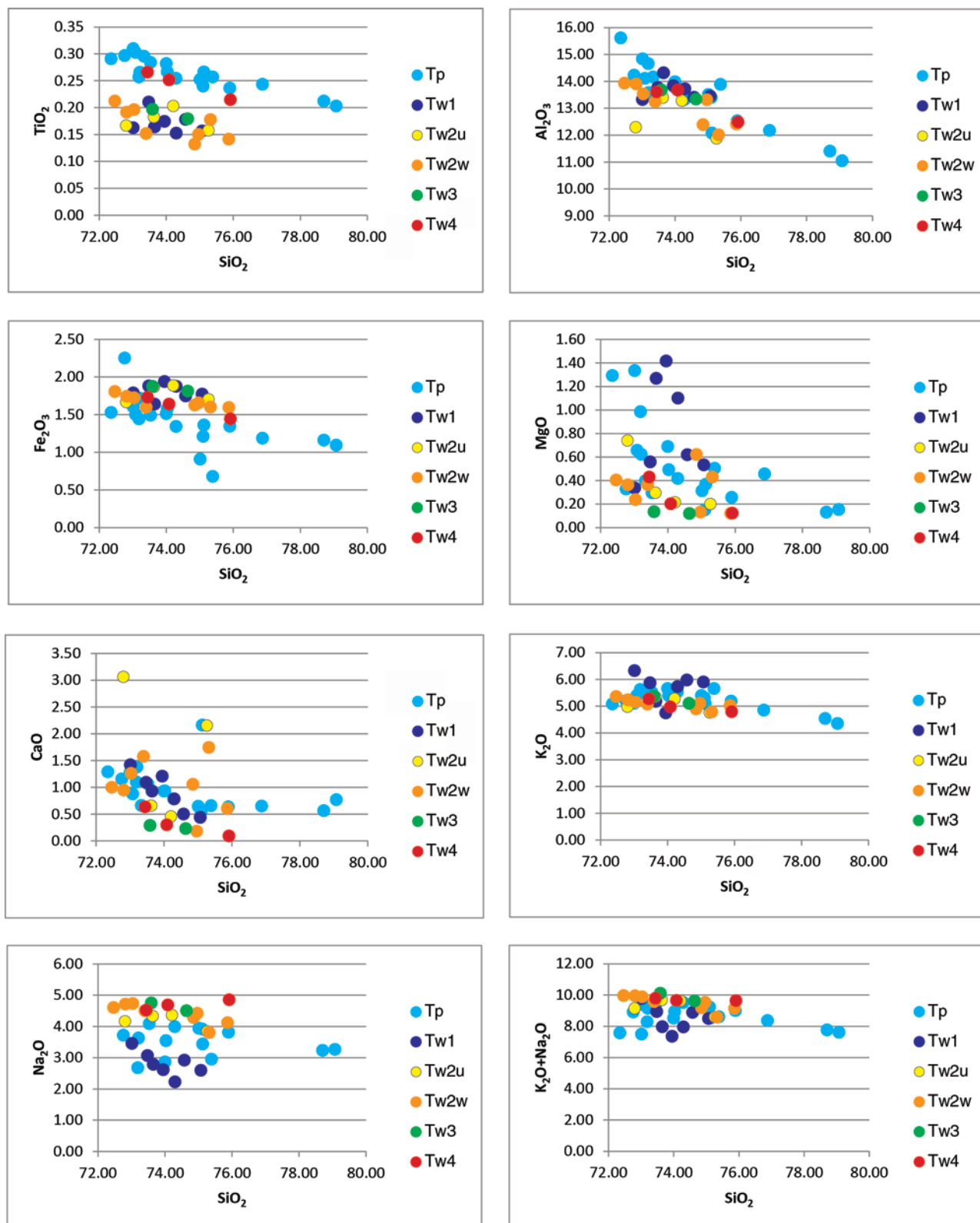


Figure 15. Harker diagrams showing variations in the abundances of selected oxides with respect to silica (SiO_2) in samples from Miocene volcanic map units Tp (Peach Spring Tuff) and Tw1, Tw2u, Tw2w, Tw3, and Tw4 (subunits of Wild Horse Mesa Tuff). Oxides are titanium (TiO_2), aluminum (Al_2O_3), iron (Fe_2O_3), magnesium (MgO), calcium (CaO), potassium (K_2O), sodium (Na_2O), and potassium + sodium ($\text{K}_2\text{O} + \text{Na}_2\text{O}$). Values are in normalized weight percent.

Appendix 4—Geochronologic Data

Nine igneous rock samples (fig. 16) were analyzed for uranium-lead (U-Pb) zircon geochronology using the U.S. Geological Survey (USGS) SHRIMP-RG (Sensitive High Resolution Ion MicroProbe–Reverse Geometry) ion microprobe at Stanford University. Zircons were separated from 2–5 kg samples using standard processing techniques. Individual zircons from mineral separates were mounted in epoxy, polished, and coated with gold prior to analysis. Relatively homogeneous spots in the rim areas of compositionally zoned zircons were selected for analysis based on cathodoluminescence (CL) images. Interior portions (cores) of the zircon crystals were not analyzed. Data were reduced and plotted using the Isoplot and Squid computer programs (Ludwig, 2008, 2009). Selected data are presented in table 6; all data are available from the SHRIMP laboratory at Stanford University. Graphic plots of the data are shown in figures 17–19.

Two samples of the Fountain Peak Rhyolite (unit *Jfr*) were analyzed. Sample 12-PR-3713 is strongly flow banded, purple rhyolite from near the southwest margin of unit *Jfr*; sample 12-PR-3889 is weakly flow banded, light-gray rhyolite near the southeast margin of the unit (fig. 12). These two samples yielded ages of 163.6 ± 1.4 and 163.9 ± 1.7 Ma, respectively; note that the age of sample 3713 is based on data combined from two separate SHRIMP runs which produced ages of 164.8 ± 2.0 and 161.3 ± 2.1 Ma. Details aside, the data clearly demonstrate a late Early to early Late Jurassic age for the previously undated Fountain Peak Rhyolite, not Miocene as originally suspected by Hazzard (1954).

Five plutonic rock samples, three of which are from different subunits of the quartz monzonite of Goldstone, were analyzed. Within the Goldstone suite, sample 12-PR-3706 from monzogranite (unit *Jgm*) west of Vulcan Mine (fig. 12) yielded the oldest age of 167.8 ± 1.8 Ma; sample 12-PR-3701 from quartz monzonite (unit *Jgqm*) farther west yielded a younger age of 163.3 ± 2.0 Ma; and sample 14-PR-5248 from quartz monzonite (unit *Jg*) near Blind Spring (fig. 12) yielded an age of 161 ± 1.9 Ma. Sample 14-PR-5021 from the monzogranite of Tough Nut Spring (unit *Jt*) 1 km north of the map area (fig. 12) yielded an age of 165.6 ± 3.0 Ma, and sample 13-PR-4854 from the monzogranite of Bonanza King Well (unit *Jbw*) in the northeastern part of the map area (fig. 12) yielded an age of 162.4 ± 2.5 Ma. Within error, the ages of all these units are very similar, and it is possible that they are all essentially coeval.

Two dikes of the felsic to intermediate suite (unit *Jdf*) were analyzed. One of these, represented by sample 12-PR-3888, is a red rhyolite dike that cuts both the quartz monzonite of Goldstone (unit *Jg*) and the Fountain Peak Rhyolite (unit *Jfr*) near sample localities 14-PR-5248 and 12-PR-3889, respectively (fig. 12). Sample 12-PR-3888 yielded an age of 162.4 ± 1.1 Ma, which is consistent with the older mean ages of the units cut by this dike. The other analyzed dike, represented by sample 14-PR-5023, is a pinkish-gray rhyolite dike that cuts the monzogranite of Tough Nut Spring near sample locality 14-PR-5021, 1.3 km north of the map area (fig. 12). Sample 14-PR-5023 yielded an age of 165.9 ± 2.4 Ma, which is indistinguishable from that of the monzogranite that it cuts.

Table 6. SHRIMP-RG U-PB zircon data for selected Jurassic igneous rock samples from the Providence Mountains in parts of the Fountain Peak and adjacent 7.5' quadrangles, San Bernardino County, California. [Title of table is included here for continuity; complete table is available at <https://doi.org/10.3133/sim3376>.]

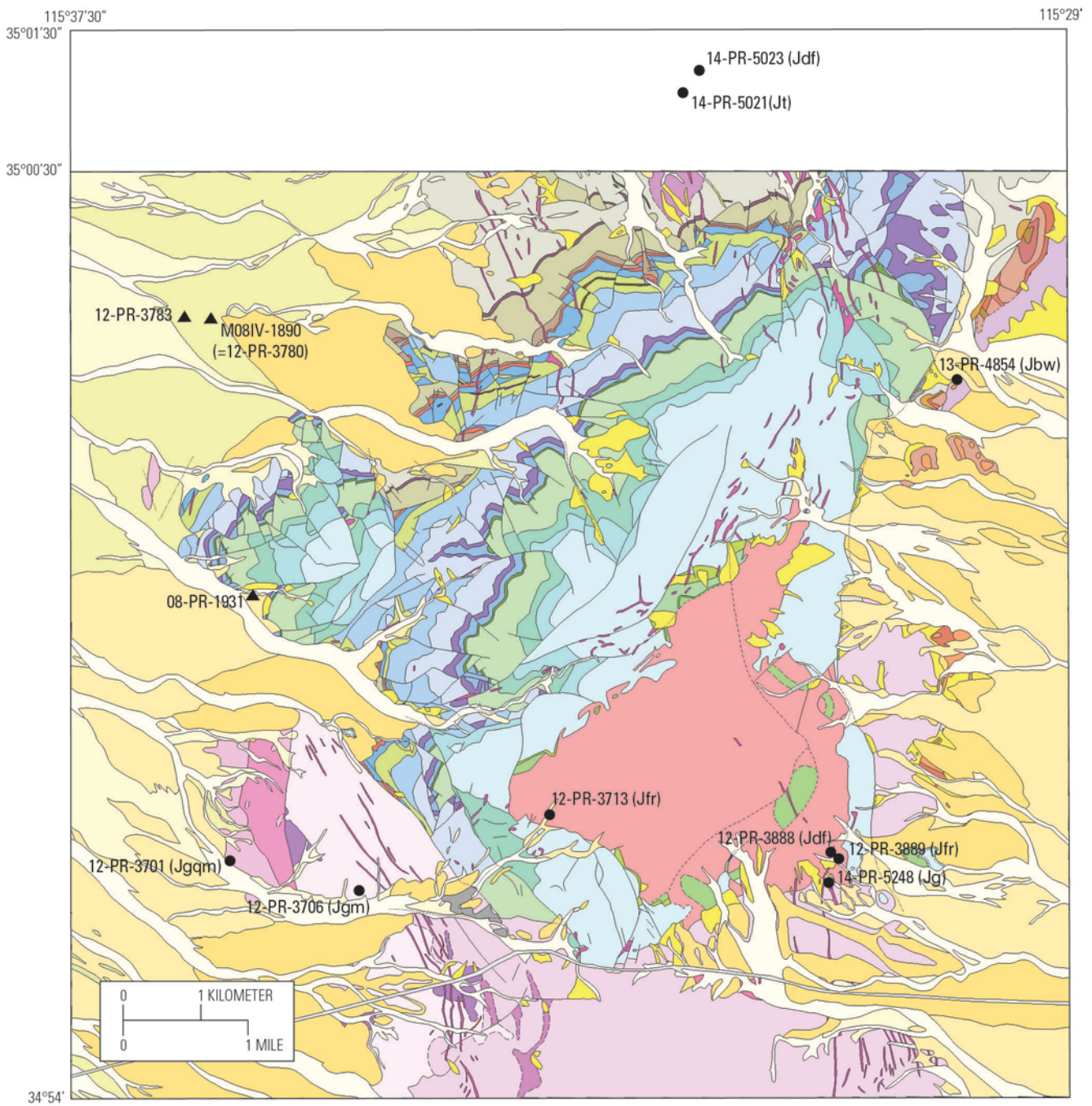


Figure 16. Reduced-scale geologic map showing locations of analyzed geochronologic samples (circles) and tephrochronologic samples (triangles). Note locations of geochronologic samples 14-PR-5021 (unit Jt) and 14-PR-5023 (unit Jdf) north of the geologic map area.

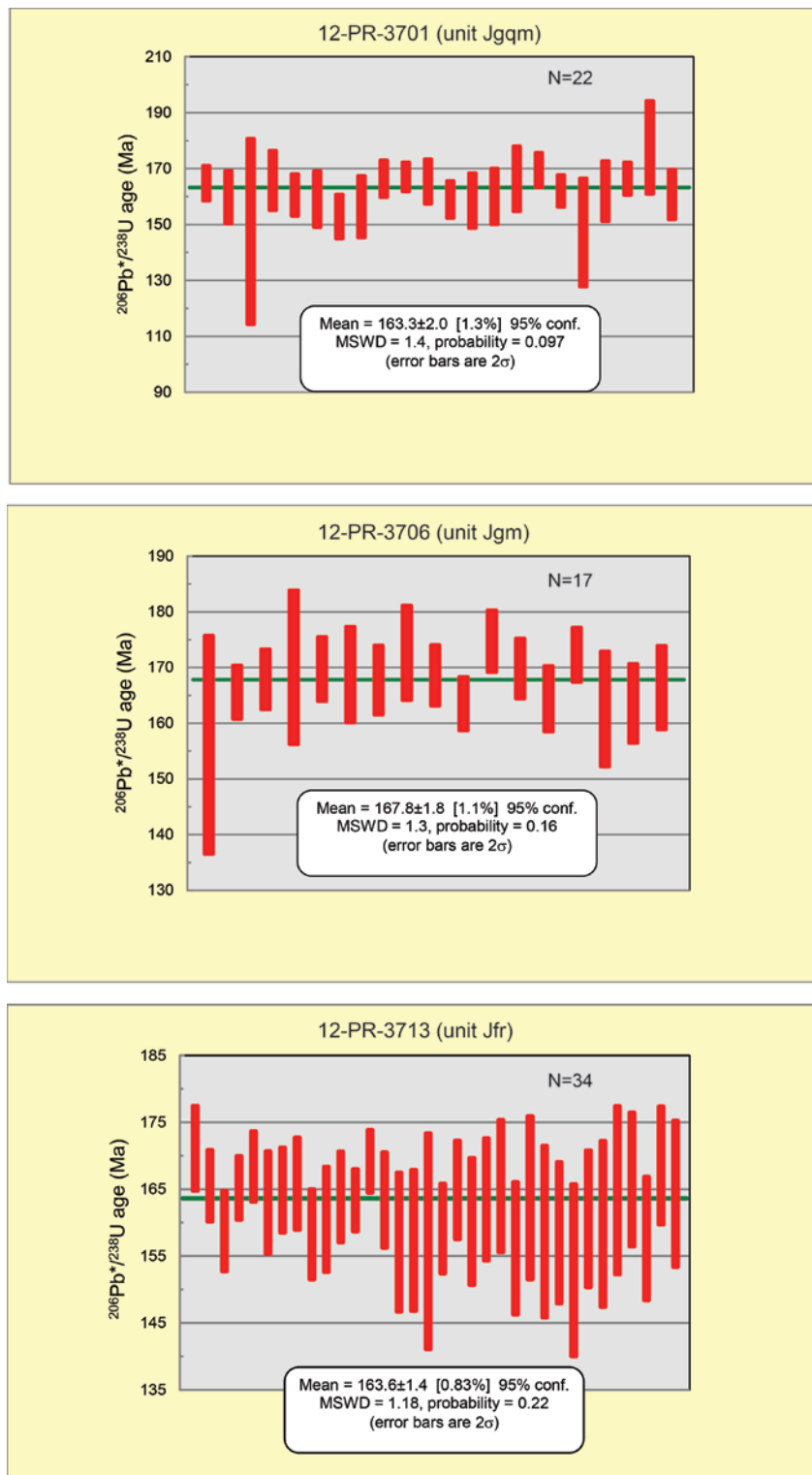


Figure 17. Weighted mean $^{206}\text{Pb}^*/^{238}\text{U}$ ages for samples 12-PR-3701 (unit Jgqm), 12-PR-3706 (unit Jgm), and 12-PR-3713 (unit Jfr). Bars depict 2-sigma errors; boxes show weighted mean crystallization ages, mean square weighted deviation (MSWD), and probability of fit. See table 6 for data.

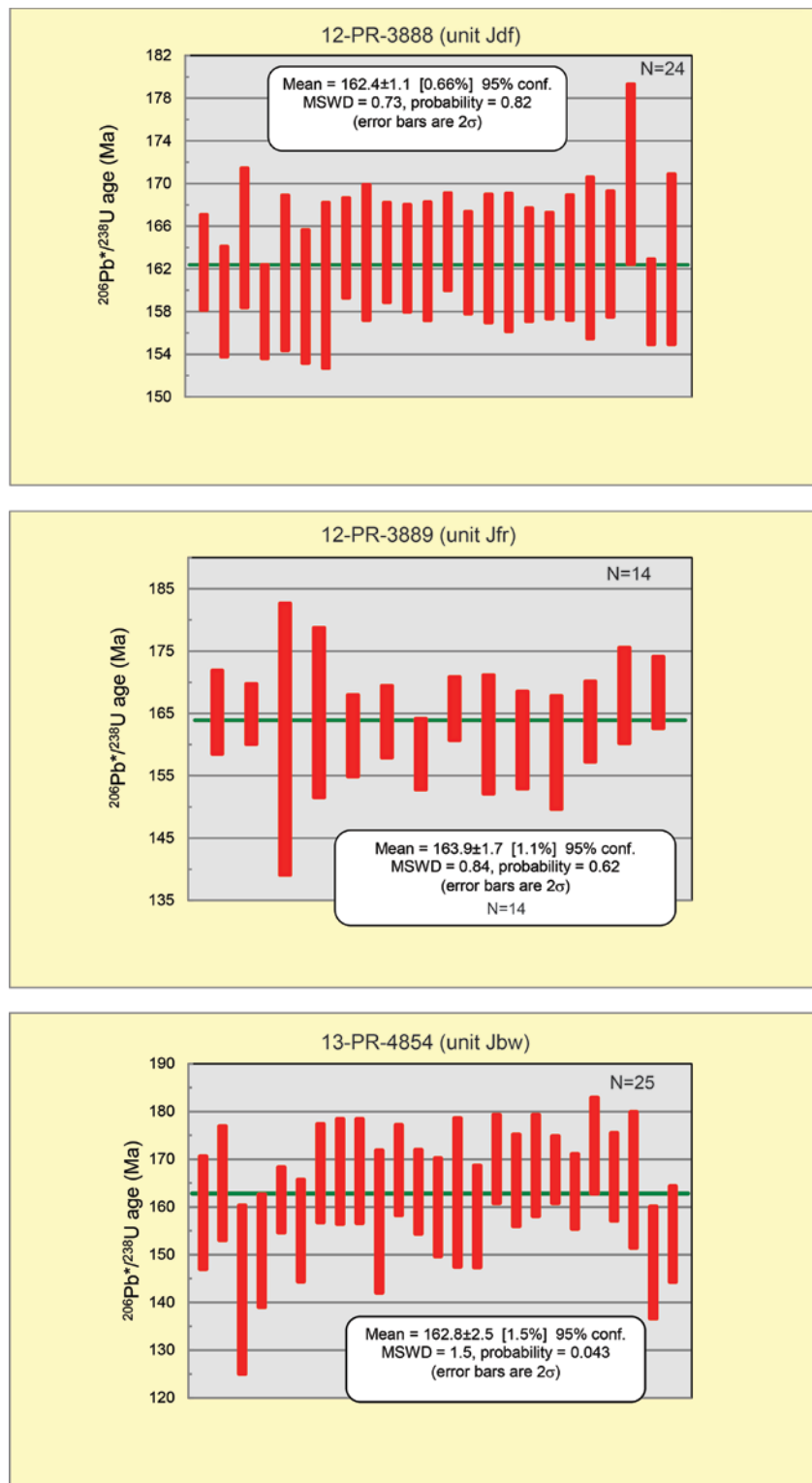


Figure 18. Weighted mean $^{206}\text{Pb}^*/^{238}\text{U}$ ages for samples 12-PR-3888 (unit Jdf), 12-PR-3889 (unit Jfr), and 13-PR-4854 (unit Jbw). Bars depict 2-sigma errors; boxes show weighted mean crystallization ages, mean square weighted deviation (MSWD), and probability of fit. See table 6 for data.

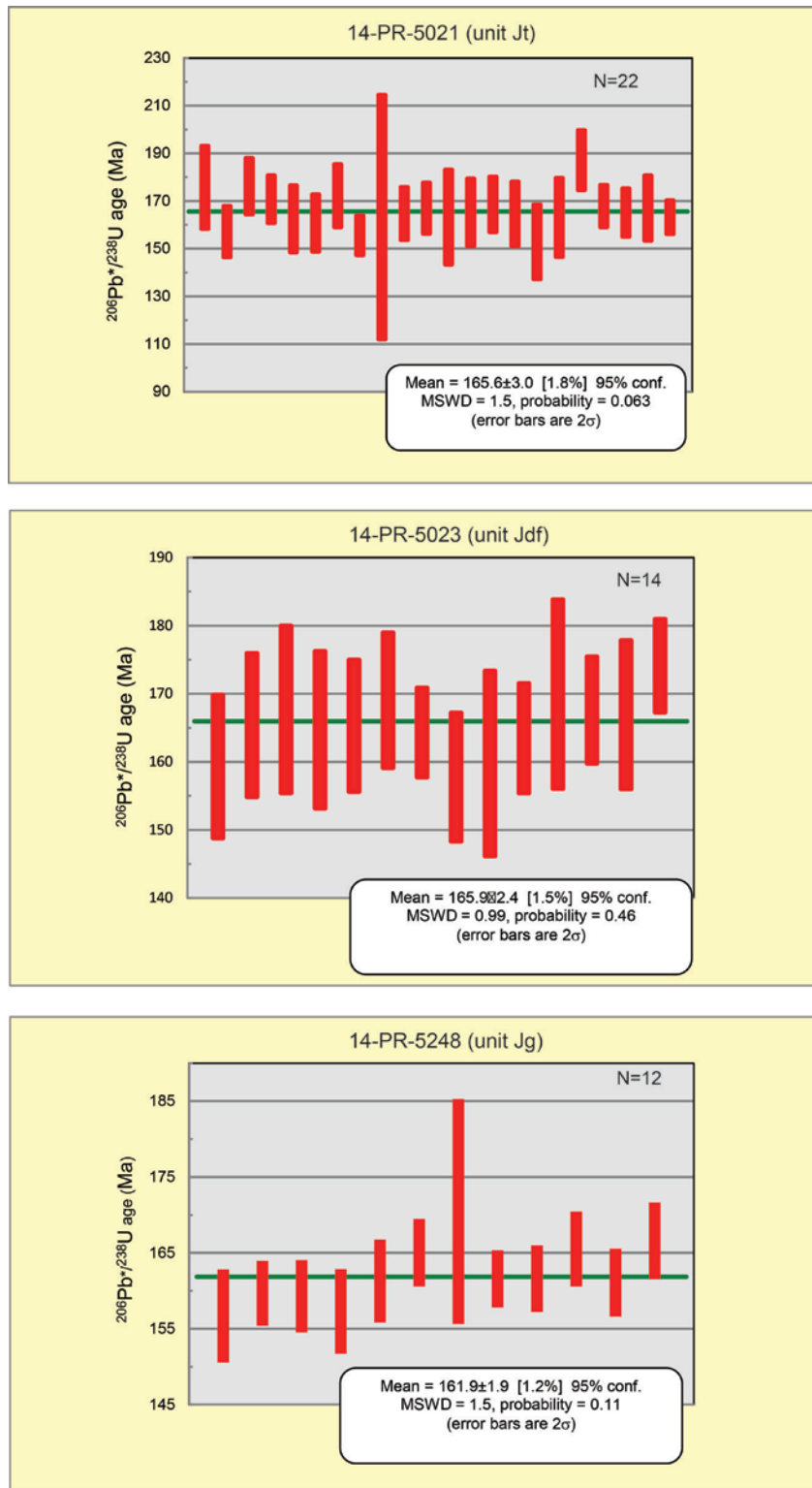


Figure 19. Weighted mean $^{206}\text{Pb}^*/^{238}\text{U}$ ages for samples 14-PR-5021 (unit Jt), 14-PR-5023 (unit Jdf), and 14-PR-5248 (unit Jg). Bars depict 2-sigma errors; boxes show weighted mean crystallization ages, mean square weighted deviation (MSWD), and probability of fit. See table 6 for data.

Appendix 5—Tephrochronologic Analysis

Introduction

This appendix summarizes the results of tephrochronologic analyses of volcanic glass in samples M08IV-1890, 08-PR-1931, and 12-PR-3783 (fig. 16; tables 7, 8) from tuffs interbedded with dissected Pleistocene alluvium on the west side of the Providence Mountains. Tephrochronology is a technique used to estimate the depositional age of an air-fall tuff, or tephra, through statistical comparison of glass composition with previously analyzed tuffs in a large database maintained by the USGS Tephrochronology Project in Menlo Park, California. Glass shards used for chemical analysis (table 8) were separated from the 200- to 100-mesh-size fraction (~75 to 150 microns, respectively) of each sample.

Table 7. Summary of chemical compositions of glass from tuff samples, Providence Mountains in parts of the Fountain Peak and adjacent 7.5' quadrangles, San Bernardino County, California, determined by microprobe analysis.

[Mean normalized oxide concentrations determined by electron microprobe analysis of glass shards. N = number of shards analyzed. See table 2 for PR sample localities. Sample M08IV-1890 was collected by D.M. Miller from same locality as sample 12-PR-3780, which is listed in table 2]

Sample	N	SiO ₂	Al ₂ O ₃	Fe ₂ O ₃	MgO	MnO	CaO	TiO ₂	Na ₂ O	K ₂ O	Total
M08IV-1890 (= 12-PR-3780)	20	78.00	13.11	0.73	0.03	0.03	0.44	0.05	3.16	4.45	100.01
08-PR-1931	20	77.99	13.14	0.72	0.04	0.04	0.44	0.07	3.19	4.38	100.01
12-PR-3783	22	77.57	13.02	0.69	0.03	0.05	0.46	0.05	3.16	4.97	100.00

Table 8. Chemical compositions of individual glass shards from tuff samples, Providence Mountains in parts of the Fountain Peak and adjacent 7.5' quadrangles, San Bernardino County, California, determined by microprobe analysis. [Title of table is included here for continuity; complete table is available at <https://doi.org/10.3133/sim3376>.]

Sample Descriptions

Sample M08IV-1890

Sample M08IV-1890 is from a lenticular bed of white tuff exposed in a deeply incised wash 0.2 km northeast of the jeep road to Cornfield Springs and 1.85 km east of the western boundary of the map area (fig. 12). The tuff lens has a maximum thickness of about 0.5 m, extends about 15 m laterally, and is about halfway up a cliff-forming section of gravelly alluvium about 15 m thick on the north side of the wash. This alluvial section is capped by a planar, darkly varnished surface mapped as intermediate alluvial deposits (unit Qia).

The sample is composed of white, well-consolidated, fine-grained, powdery ash that contains about 94 percent lightly coated, subangular to subrounded, ribbed, blocky, bubble-wall and bubble-wall-junction glass shards. Less common vesiculated shards have well hydrated, equant to irregular, bubble-

type vesicles or elongate (often conical) shapes, often displaying parallel alignment. A few shards contain aligned microlites and (or) microphenocrysts. Minor mineral grains include subhedral tectosilicates and few biotite grains. Mineral grains commonly are glass coated, and a few are slightly altered.

Sample 08-PR-1931

Sample 08-PR-1931 is from a 12-cm-thick tuff bed exposed on the north side of a low ridge of old alluvium (mapped as unit **Qoa**) in the major canyon south of Rex Mine (“Long Canyon” of Hazzard, 1954), 2.4 km east of the west boundary of the map area (fig. 12). The sample is composed of well-consolidated, yellowish-white ash together with coarser, poorly sorted clasts. The sample contains about 96 percent carbonate-coated, commonly ribbed, bubble-wall and bubble-wall-junction, blocky or well-hydrated, vesiculated/frothy glass shards. Vesicles include large, equant or irregular bubble types or elongate spindle shapes. Associated mineral grains include subhedral to anhedral, moderately to heavily altered tectosilicates and biotite, along with some grains too altered for identification.

Sample 12-PR-3783

Sample 12-PR-3783 is from the same wash as sample M08IV-1890, 0.35 km downstream (west) from that locality (fig. 12). The sampled tuff is about 30 cm thick and 1.5 m above wash level on the south side of the wash. The sample contains about 95 percent heavily coated (primarily carbonate, some clay, and iron oxides), angular to subrounded, predominantly colorless, solid, coarsely to finely ribbed glass shards. Subpopulations of light-brown, platy, bubble-wall/bubble-wall-junction, and (or) poorly to moderately vesiculated shards were also noted. Vesicles are equant type, typically slightly to super hydrated, and often show parallel orientation within ribbed shards.

Analysis

Electron microprobe analysis shows that all three samples are chemically very similar and compare closely with the upper tuffs of Glass Mountain and the Bishop Tuff of the Owens Valley area, California, about 400 km northwest of the study area, with similarity coefficients greater than 95 percent. This correlation suggests an age range of about 0.87 to 0.76 Ma for the sampled tuff layers. It seems likely that all three samples represent a single tuff deposit although the possibility that more than one deposit is present cannot be ruled out. It should be noted that the samples also resemble the 1.15 Ma Bailey ash bed and the Pliocene Mesquite Springs family of tuffs, although these tuffs contain higher concentrations of manganese.

The age of the tuff at locality 08-PR-1931 is consistent with the early to middle Pleistocene age assigned to the enclosing alluvial sediments of unit **Qoa**. By contrast, the tuff outcrops at localities M08IV-1890 and 12-PR-3783 are inferred to be significantly older than the overlying **Qia** alluvial surface of middle to late Pleistocene age. The deeply dissected alluvial section that includes these two localities evidently represents a time interval spanning several hundred thousand years.